THE EVALUATION OF AN ARGON AND HELIUM HIGHLY EFFICIENT MICROWAVE INDUCED PLASMA AS AN ELEMENT SELECTIVE DETECTOR FOR PACKED COLUMN SUPERCRITICAL FLUID CHROMATOGRAPHY

by

Curtis Bobby Motley

Dissertation submitted to the Faculty of the Virginia Polytechnic Institute and State University in partial fulfillment of the requirement for the degree of

Doctor of Philosophy

in

Chemistry

APPROVED:

Gary L. Long, Chairman

John G. Mason

James P. Wightman

Harold M. McNair

James M. Tanko

May 1990

The Evaluation of the High Efficiency Microwave Induced Plasma as an Elemental Selective Detector for Packed Column Supercrical Fluid Chromatography

by

Curtis Bobby Motley

Committee Chairman: Gary L. Long

Chemistry

(ABSTRACT)

Atomic emission spectroscopy is a powerful method for chemical analysis because it offers convenient qualitative and quantative determination of the elemental composition of an analytical sample. Although most frequently used to determine the total concentration of a given analyte, atomic spectroscopy may be coupled with a separation technique to aid in the elemental identification of individual species.

Recently, supercritical fluid chromatography (SFC) has gained popularity among the research community partially because SFC is much more tolerant of polar functional groups than is gas chromatorgraphy (GC). SFC can be used in applications where derivatization is not possible due to sample complexity or steric hindrance. However, these polar compounds often require the addition of polar organic solvents to SFC to improve retention characteristics and peak shape. These polar modifiers reduce or eliminate the utility of flame-based detectors. Therefore, researchers

have begun to look for alternative detection systems for SFC with polar modifiers.

In particular, atomic emission based detectors using plasmas have become popular to fill this void. This research stems from several characteristics that the plasma based detectors possess which make them more appealing than flame-based photometric detectors. These characteristics include improved analytical sensitivity, fewer spectral interferences, a wide dynamic range and the ability to tolerate polar organic modifiers. Possibly the most important attraction of the plasma detector is, with respect to chromatographic analyses, that this detector allows analysis of compounds that co-elute from a column because the detector is element-specific.

The evaluation of the high efficiency microwave induced plasma (HEMIP) as an elemental selective detector for packed column supercritical fluid chromatography has been explored in this dissertation. The effect of CO_2 introduction on the analytical parameters of the plasma, the feasibility of coupling packed column supercritical fluid chromatography to the argon HEMIP for the determination of metals, the use of a helium sustained plasma for nonmetal determinations, and the application of the He-HEMIP as a sensitive and selective detector for packed-column SFC.

ACKNOWLEDGEMENTS

There are so many people to thank, but I wish to first thank my parents George and Renell who gave me the encouragement and support when all others had nothing but doubt.

I offer a sincere thank you to Dr. Gary L. Long for his guidance and greatly welcomed financial support during my graduate work at Virginia Tech.

To the plasmen, here and gone, (Keith McCleary, Terry McCreary, Jeff Bolton and Larry Perkins) a special thanks for the many discussions which were sometimes helpful and scientific, while others were helpful and not so scientific.

To my other friends at Virginia Tech that allowed my graduate career to be more than just scientific.

To my lovely wife, Susan, who has been instrumental in the completion of this "experience". She offered the extra encouragement and understanding when the task at hand seemed never ending.

Finally, through Susan's and my spiritual faith each goal was met and overcame by the grace of God.

TABLE OF CONTENTS

LIST OF FIGURES

LIST OF TABLES

Chapter 1

INTRODUCTION

Atomic emission spectroscopy is a powerful method of chemical analysis in that it offers convenient qualitative and quantitative determination of the elemental composition of an analytical sample. Although most frequently used to determine the total concentration of an element in a specific sample, atomic spectroscopy can be coupled with a chromatographic technique to aid in the elemental identification of separated analyte species.

The focus of this study is to investigate the coupling of a supercritical fluid chromatograph, SFC, to a microwave induced plasma, MIP, for the purpose of performing elemental specific detection on the eluting chromatographic peaks. This study will explore the coupling of the two techniques by examining: the effect of the introduction of CO_2 on the analytical parameters of the plasma; the use of various torch designs for sample introduction; the use of an Ar sustained plasma for metal determinations; the use of a He sustained plasma for nonmetal determinations; and the application of SFC-MIP to the determination of industrial samples. To place this study in perspective, a review of microwave cavities and their use in chromatography will be

presented. Also, the use the high efficiency MIP employed in this study will be discussed.

Beenakker Cavity

Historically, the development of the TM_{010} microwave resonant cavity by Beenakker in 1979 [1] has provided the atomic spectroscopist with a stable and efficient means for generating a low powered (<200 W) microwave induced plasma (MIP) which is capable of operating at reduced or atmospheric pressure with a variety of support gases (Ar, He, and N_2). Although very flexible with respect to the composition of the support gas, the Beenakker design was unable to tolerate the introduction of an aerosol from conventional plasma nebulizers/spray chambers. This limitation precluded the use of the cavity from samples that were otherwise performed by inductively coupled plasma emission spectrometry.

Non-aqueous Sample Introduction

A strength of this cavity over other plasma sources was the small flow rate of gas needed to support the plasma. Researchers [2-6] quickly realized the potential of coupling the Beenakker cavity to a gas chromatograph (GC) for the purpose of elemental detection of the eluent. The interface permitted the researcher to circumvent the significant

problem of sample introduction in the microwave cavity. For a typical analytical determination, the solvated analyte is introduced into the plasma discharge. Here the processes of desolvation, vaporization, molecular dissociation, and excitation occur. Although the MIP possesses excitation temperatures in the 3000-4000 K range, the plasma could not tolerate solvated samples. However, with the GC-MIP system, the analyte is delivered to the MIP as a gas (diluted in He), thus requiring the plasma discharge to only dissociate and excite the analyte vapor. This union of techniques provided the analytical chemist with the means of on-line separation and elemental speciation of the analyte. The potential analytical power of this system has been recognized by Hewlett-Packard, which introduced a GC-MIP atomic emission detector in 1989 after years of research and development into element selective detectors for GC.

Alternate methods [7] of sample introduction were being employed concurrently. These methods (chemical hydration and electrothermal vaporization) work well with the Beenakker cavity because, as with GC introduction, two major energy consumption steps (desolvation and vaporization) of the atomic emission process have been eliminated prior to the plasma. However, the Beenakker design lacked the ability to excite aqueous samples adequately as the cavity was not critically coupled in that the microwave power from

the generator was not being efficiently channeled into the resonant cavity to maintain the plasma discharge.

High Efficiency Microwave Induced Plasma

In order to overcome the problem of power transfer to the cavity Boss et al. [8] through the use of a movable antenna or probe modified the Beenakker design to couple the microwave induced plasma with the generator more efficiently . This probe could be moved along the radial face of the cavity to sense a position of 50 ohm impedance. Unlike the Beenakker design which had a fixed probe position and relied on the use of external resistive loads to adjust the impedance to 50 ohms. Boss et al. [8] stated, "cavity coupling refers to an interaction between systems such that effects in one system produce effects in the other."

The concept of coupling in a MIP system is important since the efficiency at which power is transferred to the cavity is related to the degree of coupling. In this system, the concern was to effectively couple two isolated electrical systems, namely a microwave generator and a resonant cavity. The objective was to deliver all the available power to the resonant cavity without loss and without reflecting any power to the generator. A resonant cavity that is critically coupled to the generator is desirable for three reasons. First, as previously

mentioned, no power is reflected from a critically coupled resonant cavity, thus extending the lifetime of the microwave generator, as the magnetron may be damaged if too much power is continuously reflected from the resonant cavity. Second, if there is no reflected power the cavity will not heat, thus eliminating the need for elaborate cooling systems for the resonant cavity. Lastly, and most importantly, a critically coupled cavity allows accurate measurement of power transferred to the plasma, which plays an important role when comparative analyses are attempted between laboratories. This coupling mechanism of the MIP to the generator, as described by Boss, results in a system which operates at nearly 100% efficiency with respect to power transfer [8].

Aqueous Sample Introduction

The Beenakker design was evaluated as a potential excitation source for aqueous solution [9, 10] due to its success as an elemental selective detector for gas chromatography, However, samples had to be desolvated or employ powers as high as three kilowatts [11] had to be employed without any gain in analytical sensitivity or selectivity. Due to the absence of critical coupling in these systems, water cooling of the cavity was required and short lifetimes (<0.7 hrs) for their torches resulted.

Later, the modified design of the Beenakker cavity by Boss et al. [8], termed the high-efficiency microwave-induced plasma (HEMIP), was employed by Long and Perkins [12-14] to analyze aqueous samples. They reported that the direct introduction of aqueous metal and nonmetal samples into a low-power MIP could be achieved with the use of a HEMIP cavity employing argon or helium as the plasma support gas, respectively.

It has been noted sample introduction limits the performance of plasma atomic emission [15, 16]. Conventional nebulizer/spray chamber systems allow less than 2% of the sample entering the nebulizer to reach the plasma, because the majority of the sample consists of droplets too large to be easily atomized. Even with this limitation atomic emission spectrometry is a powerful method for chemical analysis in that it offers convenient qualitative and quantitative determination of elemental composition of a sample. Although most frequently used to determine the total concentration of a given analyte, atomic spectrometry can be coupled with a separation technique to aid in the elemental identification of individual species.

Supercritical Fluid Chromatography

During the past several years interest in supercritical fluid chromatography (SFC) has increased. SFC requires a

supercritical fluid mobile phase which is a gas that has been heated to a temperature above its critical temperature and simultaneously compressed to a pressure above it critical pressure to a homogeneous, dense fluid with solvent properties different from those of gas and liquid states. The solvating properties of the supercritical fluid depend greatly on its density. Carbon dioxide, the most widely used supercritical fluid, has properties somewhat like those of a gas when its density is low or those of a liquid when its density is high. Therefore, changing the density of a supercritical fluid, which is done by increasing the pressure, changes its solvating ability and therefore the retention time of the sample components. Supercritical fluids have viscosities which are more typical of gases than liquids and diffusion coefficients intermediate between those of gases and liquids. Thus, interest in SFC has been generated because the use of supercritical fluids as mobile phases in chromatography allows fast and high resolution separations of many less volatile or thermally labile compounds not amenable to gas chromatography. Another advantage of SFC over GC is the availability of a variety of fluids as mobile phases that offer a range of polarity and selectivity, such as is found in liquid chromatography.

Theoretically, any substance that is stable above its critical temperature and critical pressure can be used as a

mobile phase in SFC. However, most current SFC practice has been limited to the use of carbon dioxide. CO_2 is a useful mobile phase in SFC because it is nontoxic, nonflammable, and compatible with a variety of conventional GC and LC detectors, such as flame ionization and ultraviolet spectroscopy. In addition, because carbon dioxide is gaseous at ambient conditions, it is suitable for interfacing to other spectroscopic instruments. However, carbon dioxide is not the ideal fluid for all possible applications of SFC as it eliminates the possibility of determining carbon and oxygen concentration of the analyte with this system.

Most recently, SFC has gained popularity among the research community partially because SFC is much more tolerant of polar functional groups than is GC. It can be used in many applications where derivatization is not possible due to sample complexity, steric hindrance, or other reasons. However, these types of compounds often require the addition of polar organic solvents to improve retention characteristics and peak shapes.

Supercritical Fluid Chromatography Detection

Although the flame ionization detector (FID) has been studied by many researchers for SFC [17-22], the FID has limited SFC separations because of its inability to tolerate

polar modifiers. Researchers [23] have stated that the use of modifiers makes the use of flame ionization detection almost impossible, although, levels of up to 1% of methanol in carbon dioxide have been reported to be compatible with FID at reduced sensitivity [16]. Therefore, researchers have begun to look for alternative detection systems. Taylor and coworkers [24] have reported that practically all investigations have been conducted on organic samples, even though the first reported SFC separation dealt with organometallic compounds. Additionally, less than a dozen reports have appeared regarding separations of metal-containing species throughout the past 25 years of SFC development. This low number of publications could possibly be due to the lack of an element selective detector.

With these two limiting factors in mind, atomic emission based detectors [25-29] using plasmas have been employed to fill the void. This research interest stems from several characteristics that the plasma based detectors possess which make them more appealing than flame-based photometric detectors. These characteristics include improved analytical sensitivity, fewer spectral interferences, a wide dynamic range and the ability to tolerate polar organic modifiers. Possibly the most important quality of the plasma detector is with respect to chromatographic analyses, in that this detector will

tolerate co-elution of two compounds from a column because the detector is element-specific [3].

Most recently, Motley and Long [17] established the feasibility of using the HEMIP as an elemental selective detector employing packed column SFC. In their work, as well as works of Hieftje et al. [24] and Jinno et al. [16] mention was made of detector "spiking" due to the "freezing" of the restrictor tip. Because of the Joule-Thompson effect of the expanding CO_2 gas, the freezing of the effluent in the restrictor tip can occur and lead to the subsequent blocking of the restrictor. After sufficient pressure builtup in the system, the blockage is dislodged and effluent streams into the plasma to form a "spike". To prevent this freezing of the restrictor, the tip is usually placed in close proximity of the plasma discharge and/or the plasma gas is heated and/or the restrictor tip itself is heated.

The evaluation of the high efficiency microwave induced plasma as an elemental selective detector for packed column supercritical fluid chromatography will be explored in the dissertation. The areas of focus will include: (1) the effect of CO_2 introduction on the analytical parameters of the plasma; (2) the feasibility of coupling packed column supercritical fluid chromatography to the argon HEMIP for

the determination of metals; (3) the use of a helium sustained plasma for nonmetal determinations; and (4) the application of the He-HEMIP as a sensitive and selective detector for packed-column SFC.

Chapter 2

EXPERIMENTAL CONDITIONS

Reagents

All chemicals used were analytical reagent grade and dissolved in distilled/deionized water or in chromatographic grade solvent. Stock solutions for all aqueous samples were purchased as 1000 ppm (Buck Scientific, Inc.) or prepared according to standard procedures [30]. Samples which used the chromatographic grade solvent were prepared by dissolving the sample in the solvent to obtain 1000 ppm with respect to the analyte of interest. Volumetric dilutions were performed to obtain the desired concentrations.

Carbon dioxide for the mobile phase was purchased as chromatographic grade (Scott Specialty Gases, PA) with a helium headspace of 1500 psi and dip tube [31, 32]. All samples were prefiltered via 0.5 um teflon filters (Fisher Scientific, NC). The plasma gases were Airco analytical grade argon and helium.

SFC Instrumentation

The CO_2 was prefiltered through a 0.5 um stainless-steel frit filter prior to the filling of the SFC pump (Suprex SFC/200A) which has a 200 mL capacity.

DeltaBond phenyl and DeltaBond cyano columns (Keystone Scientific, PA) used in these studies have an inner diameter of 1 mm and were 10 cm long with 5 um particles.

Injections were performed with a high-performance chromatography Rheodyne Model 7250 valve (Cotati, CA) equipped with a 0.5 uL injection rotor. In order to eliminate band broadening at the injector point, the head of the column was placed as close as possible to the injection rotor. All injections were performed in a splitless manner. The entire injection apparatus was mounted outside the oven, to allow injections to be made at room temperature.

In order that elemental detection at atmospheric pressure could be accomplished, a tapered restrictor was employed [33]. The restrictor was fashioned in-house and pulled from 50 um fused silica to an orifice approximately 10 um. The restrictor was inserted into the plasma torch through a septum and placed either 1 cm directly below the plasma plume (Figure 1) or inserted into the sidearm of the torch (Figure 2).

Sample Introduction.

Samples were introduced into the plasma one of three ways: (1) aqueous nebulization; (2) supercritical fluid effluent through the central portion of the microwave torch;

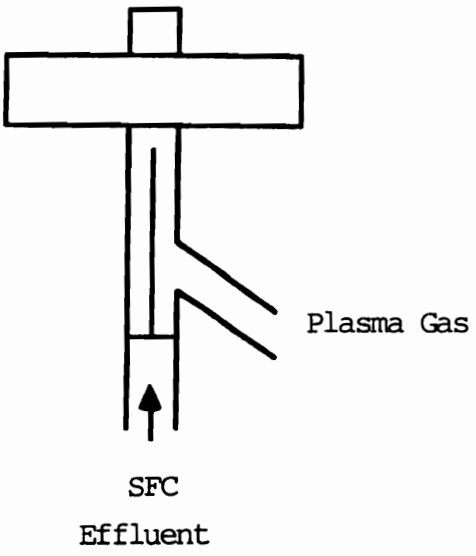

Figure 1: Central Introduction of SFC Effluent into the HEMIP

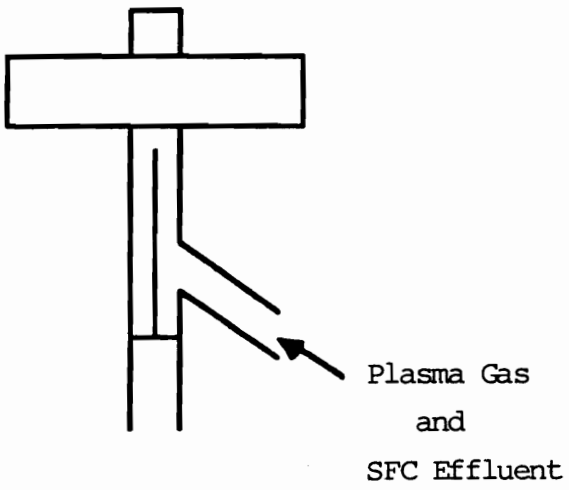

Figure 2: Sidearm Introduction of SFC Effluent into the HEMIP

or (3) supercritical fluid effluent through the sidearm of the microwave torch.

Aqueous nebulization employed a typical ICP-AES pneumatic nebulizer/Scott-type spray chamber system. A diagram of this combination sample introduction system is shown in Figure 3. All aqueous nebulization was employed solely to find the analyte emission line of interest.

Sample introduction via supercritical fluid effluent through the central portion of the microwave torch consisted of the tapered restrictor (8 mm I.D.) being positioned in the central tube of the torch and placed approximately 1 cm below the plasma plume. This configuration is shown in Figure 1. This arrangement proved to be somewhat troublesome, since the restrictor would occasionally "freeze" when the CO_2 decompressed, thus causing detector "spiking". More importantly, great caution had to be exercised to prevent the plasma from arcing back on the restrictor. If arcing occurred, the result would be fusion of the tip. In another work Hieftje et al. [27] also noted the fusion phenomenon to occur. In addition, this central arrangement required approximately two times the argon flow as compared to sidearm introduction to maintain a centered plasma within the torch.

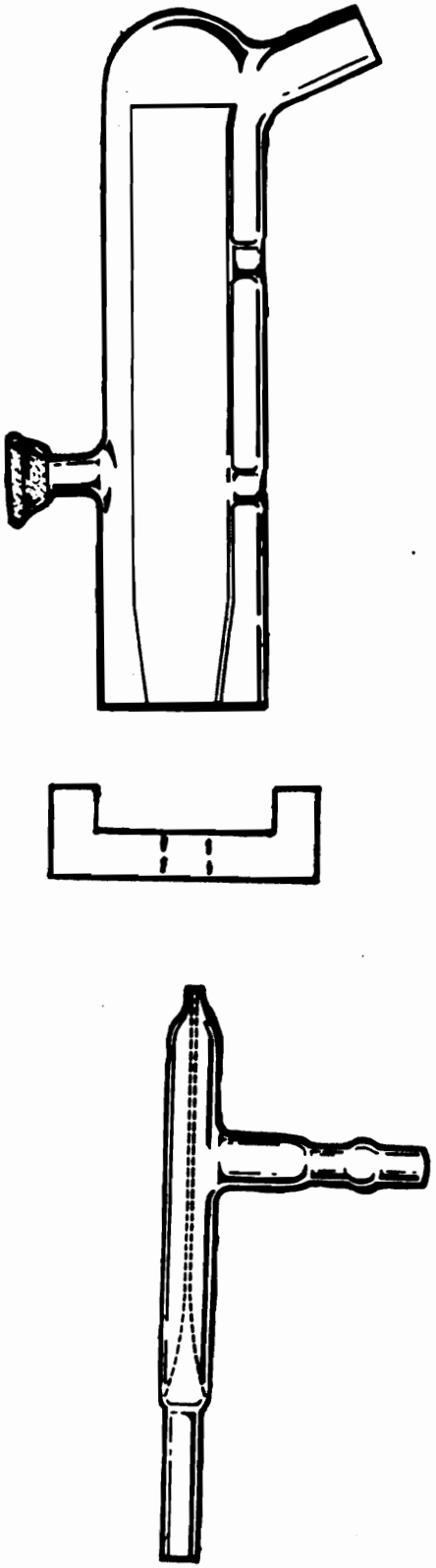

Figure 3: Aqueous Sample Introduction Nebulizer/Spray Chamber

The final sample introduction method placed the restrictor in the sidearm of the torch where the effluent gas was premixed with the plasma support gas, as shown in Figure 2. This arrangement did not demonstrate restrictor "freezing", because the plasma gas flow was at a right angle (Figure 4) to the restrictor tip thus preventing the nucleation of CO_2 as it decompressed. Also, arcing by the plasma did not occur, eliminating the possibility of the restrictor being fused. An additional benefit of this type of introduction is the premixing of the effluent with the plasma gas prior to encountering the plasma discharge. This mixing permitted the plasma gas flow rate to be reduced, resulting in a more stable plasma discharge.

Microwave Cavity

A generic schematic of the TM_{010} microwave resonant cavity by Beenakker [1, 2] is shown in Figure 5. The microwave resonant cavity chosen for this work is shown in Figure 6. This design is a modification of that described by Boss et al. [8], since this new cavity was designed especially for the helium plasma. The internal diameter of the cavity is slightly larger than that described by Boss et al. [8] and the total volume of quartz is greater. Other changes include a change in overall size and reconstruction of the probe translation stage. Figure 6 is a diagram of

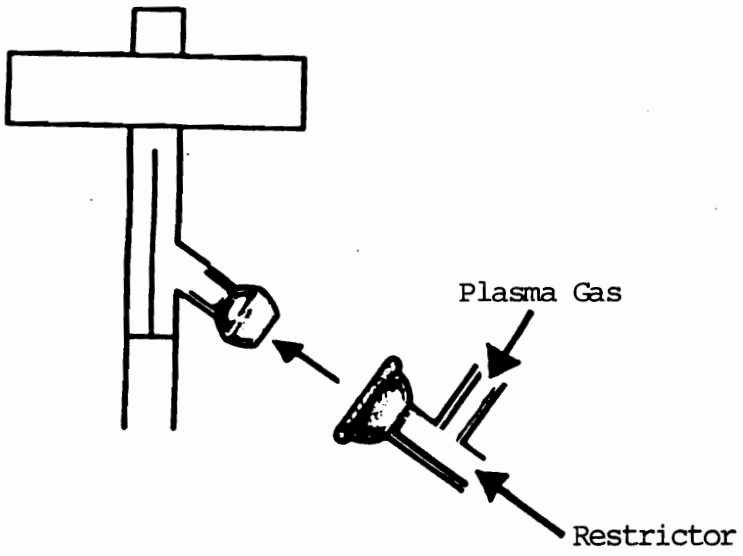

Figure 4: Restrictor/Plasma Gas Right Angle Configuration

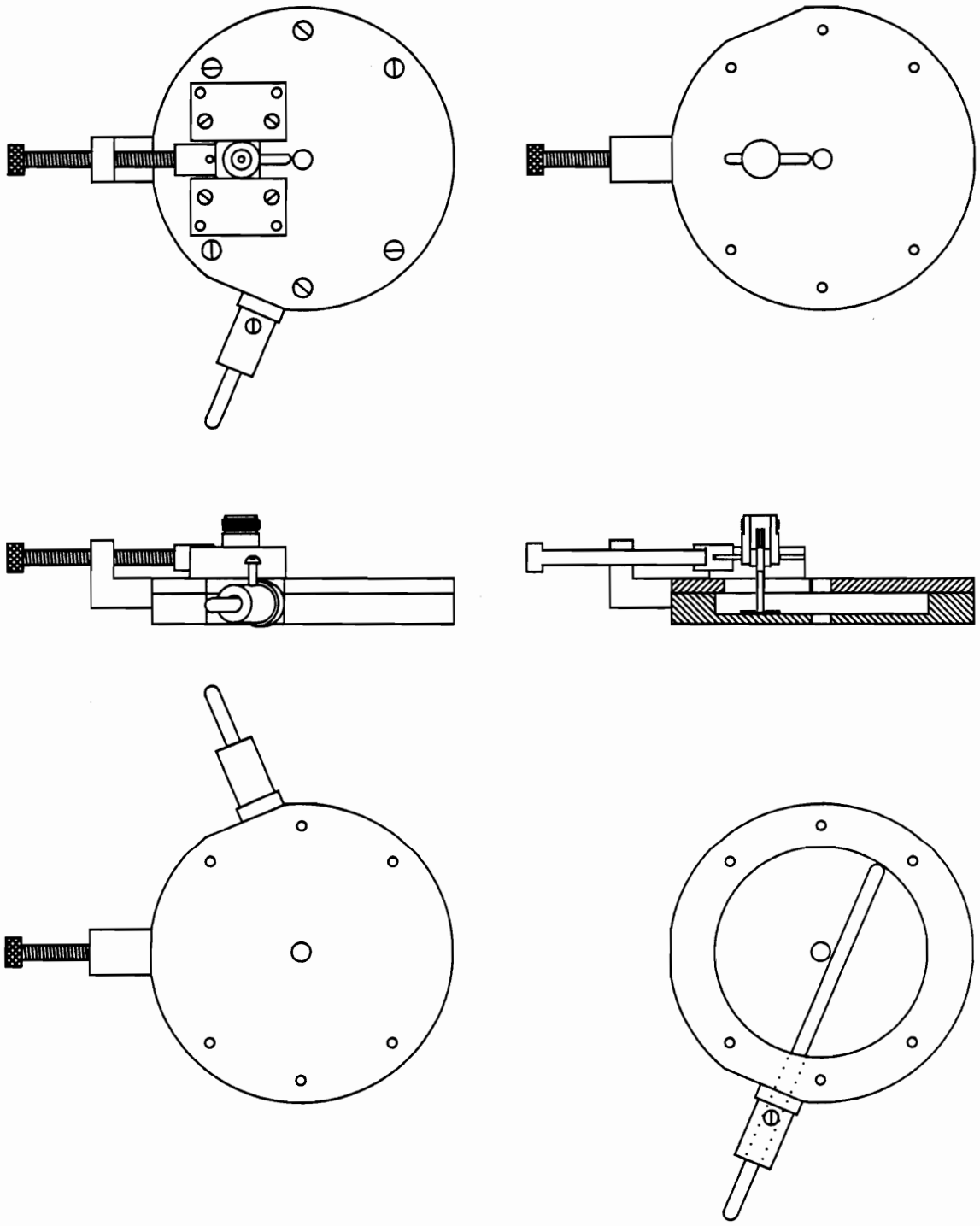

Figure 5: Schematic of the TM_{010} Highly Efficient Microwave Resonant Cavity (Computer Graphics by Mark Wingerd)

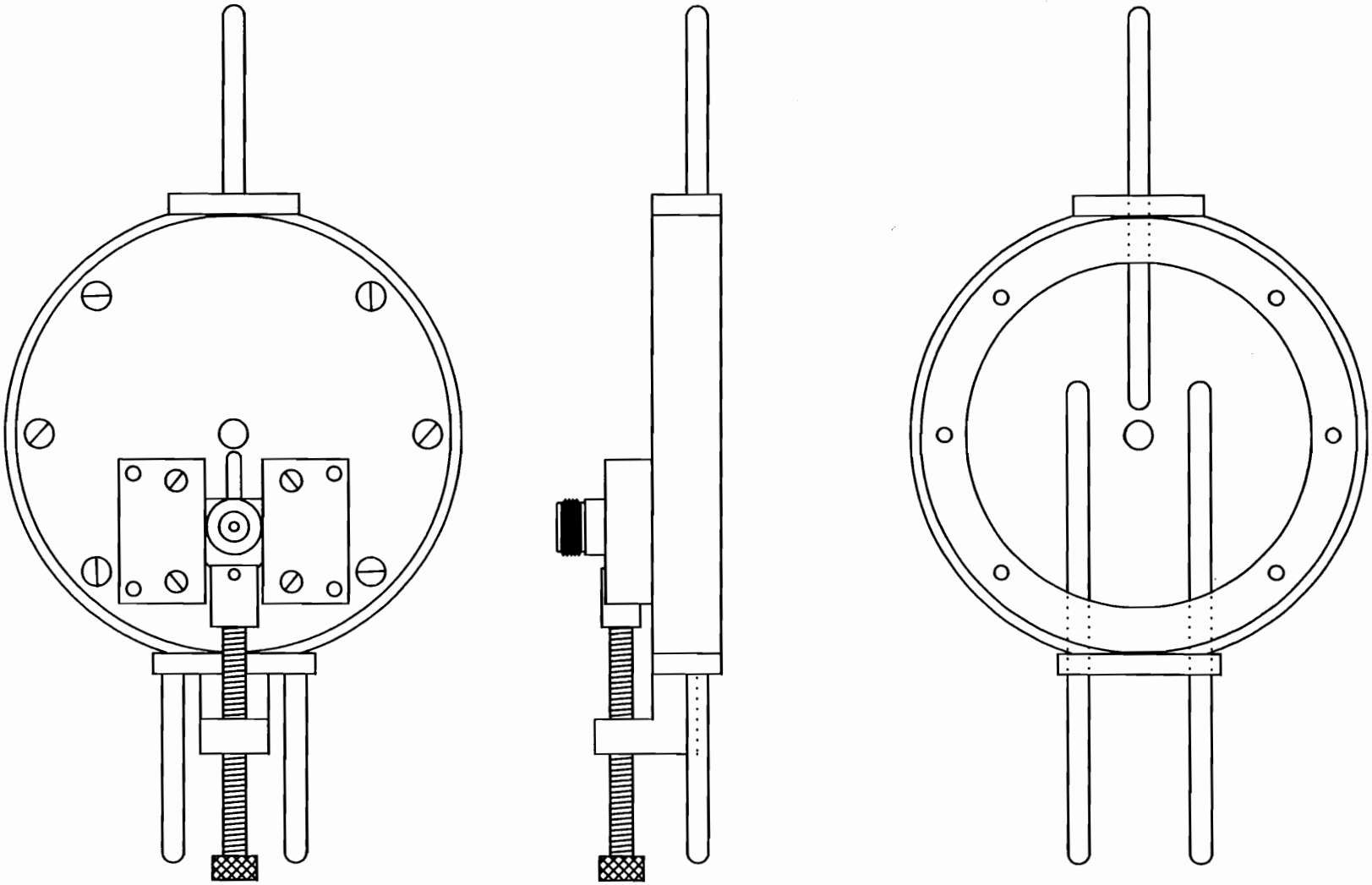

Figure 6: Schematic of the Modified TM_{010} Highly Efficient Microwave Resonant Cavity
(Computer Graphics by Mark Wingerd)

the cavity body emphasizing the major changes. The cylindrical cavity was machined from an one inch thick sheet of oxygen free high conductivity copper (OFHC). The inner diameter and depth of the cavity were fixed at 96.0 mm and 10.0 mm, respectively. Three-eight mm diameter quartz rods extended into the cavity through the side wall with teflon screws machined to secure them in place once the plasma had been critically coupled with respect to the cavity resonant frequency to the generator frequency (2450 MHz).

A removable lid was machined to 0.197 inches using a two inch sheet of OFHC. An eight millimeter diameter hole was drilled into the center of the lid and cavity to facilitate insertion of the plasma discharge tube. A 0.196 X 1.570 inch radial slot was machined along the translation axis. This allowed lateral movement of the capacitive antenna coupling probe. This movement allowed the 50 ohm impedance of the cavity to be located. This step, as well as the frequency matching step allowed the cavity and generator to be "critical coupled" [8].

The antenna probe was made from UG 58 A/U type N coaxial connectors as describes by Boss [8, 34]. A ten gauge copper wire was silver soldered to the center post of the N connector and a 16 mm diameter copper disk was silver

soldered to the end of the copper wire. Sheet metal shims were used to adjust the probe penetration depth to 96%.

MICROWAVE TORCH

A centered plasma was produced using a tangential flow torch similar to that employed in ICP-AES [34]. The microwave torch used in all studies consisted of two concentric quartz tubes (see Figure 7). The dimensions of the outer tube were 6 mm i.d., 8 mm o.d. and 9 cm long. The dimensions of the inner tube were 1.5 mm i.d., 2 mm o.d. and 2.5 cm long.

Plasma Ignition and Operation

The plasma was sustained with a 1 L/min gas flow, which was introduced through the side inlet of the plasma torch with a pressure of 50 psi of gas. There was an auxiliary argon flow of 2 L/min (40 psi) introduced in a tangential fashion to the torch, which allowed the plasma to stay centered within the torch when the SFC effluent was introduced through the central portion of the torch (Figure 1). But this auxiliary flow was not employed when the effluent was introduced through the sidearm of the torch (Figure 2).

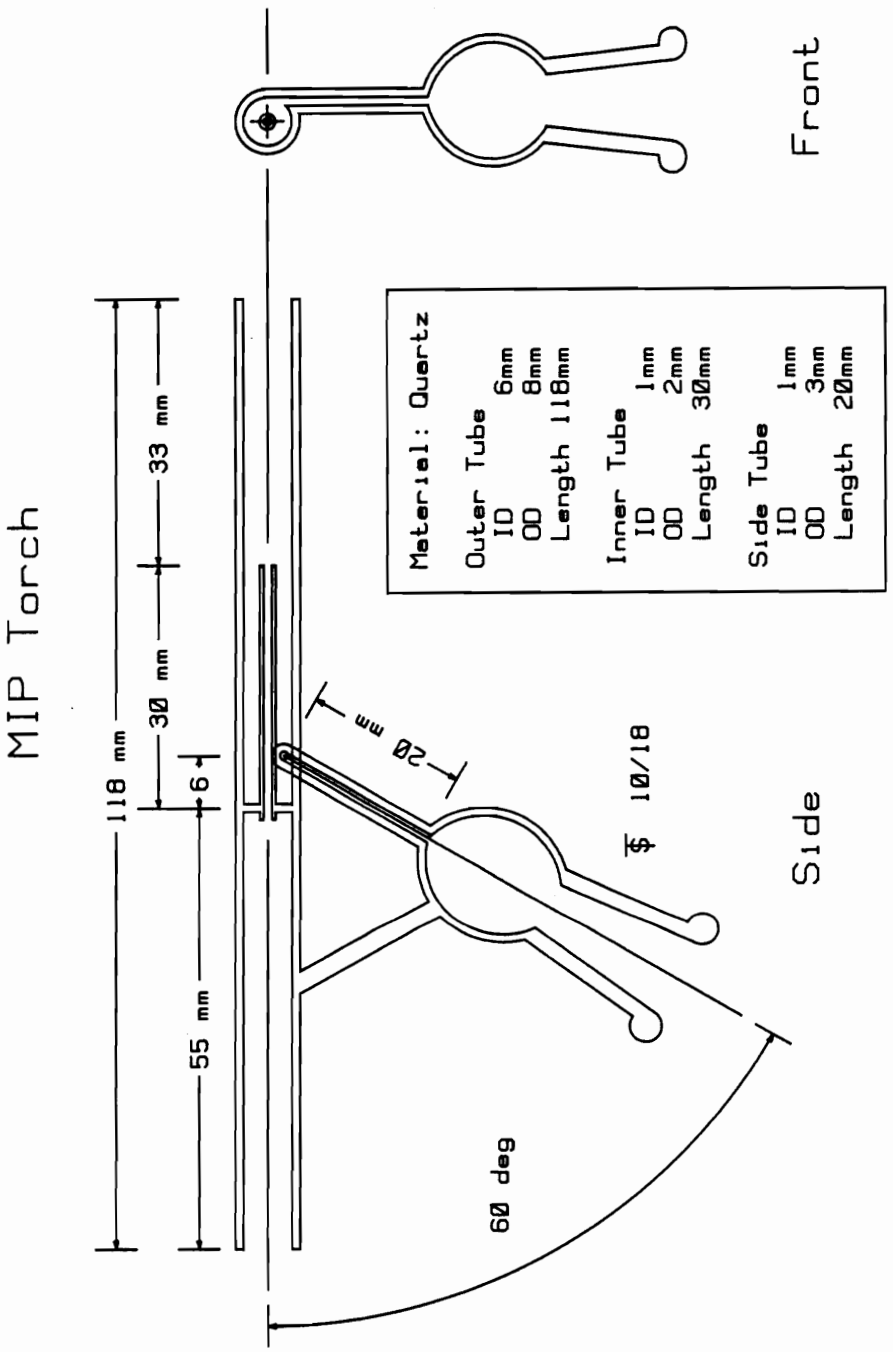

Figure 7: Schematic of the Microwave Torch (Computer Graphics by Mark Wingerd)

The applied power to the cavity was 150 W. The plasma was ignited by inserting a tungsten wire attached to a rubber policeman, for insulation and safety of the operator, into the quartz torch within the TM_{010} cavity. This insertion allowed the wire to be inductively heated by the field, causing a "seed" of the plasma gas to ignite the plasma. The plasma was tuned to 0 W reflected power by adjustment of a sliding quartz rod and by utilization of the electrical properties of an antenna probe [8].

The optimum operation parameters employed for the central and sidearm introduction are shown in Table 1. These parameters were chosen after changing one parameter at a time to obtain the maximum S/N ratio.

Optical System

The atomic emission data obtained for this work was performed in the radial or axial mode. These two modes are shown in Figure 8 and Figure 9, respectively. Table 2 lists all of the optical, electrical, and gas handling equipment with their manufacturers.

Emission from the plasma was focused onto the entrance slit of a 0.25 m monochromator using a f/3 suprasil lens to obtain one-to-one imagining. Current signals resulting from analyte emission were collected using a R955 Hamamatsu PMT

Table 1: Operational Parameters for SFC-MIP-AES

Forward Power	150 W
Reflected Power	0 W
Observation Height	
Radial	0.5 mm
Axial	0.0 mm
Plasma Support Gas	
Argon	1.8 L/min
Helium	1.0 L/min
Auxilary Flow	
Central (Ar Only)	1.2 L/min
Sidearm (Ar)	0 L/min
Sidearm (He)	0 L/min
Probe Penetration	96 %

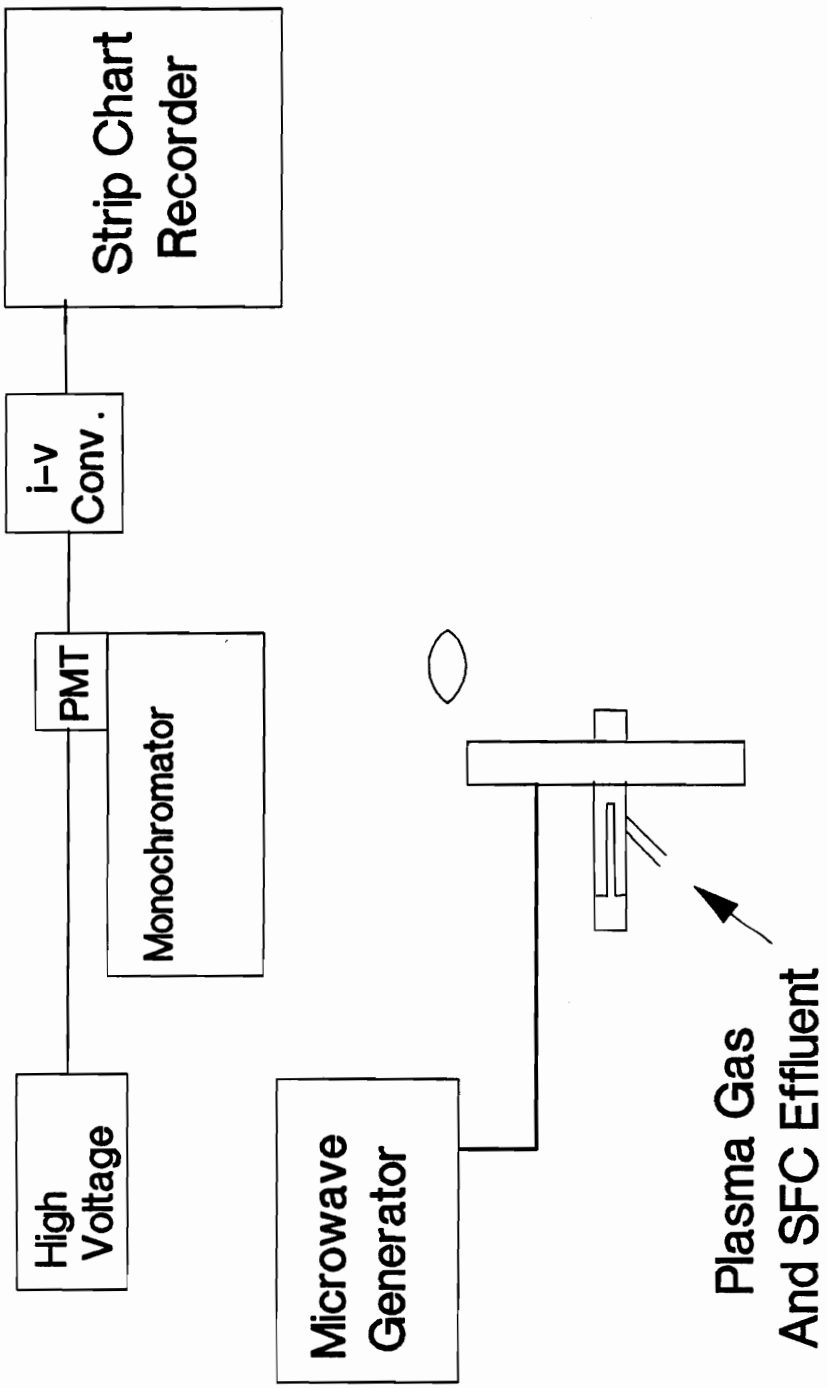

Figure 8: Block Diagram of the Radial Mode Apparatus

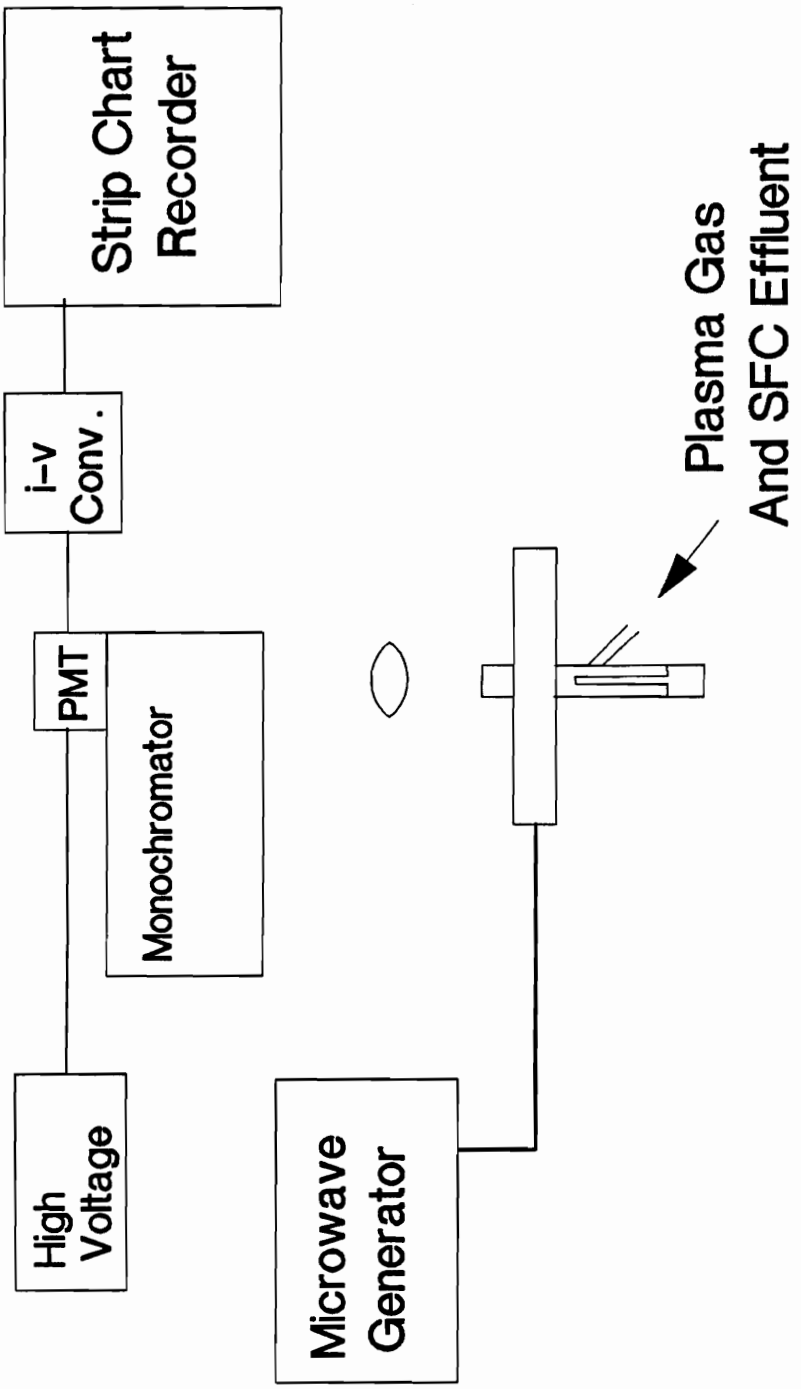

Figure 9: Block Diagram of the Axial Mode Apparatus

Table 2: Equipment Used in SFC-MIP-AES

Components	Model / Size	Manufacturer
Microwave Cavity	Highly Efficient TM(010)	Laboratory Built
Generator	HI-2450	Holaday Ind. Edina, MN
Discharge Tube	Tangential Flow	Laboratory Built
Coaxial Cable	50 ohm, RG-214	Time Fiber Communications Wallington, CT
Monochromator	01-512, 0.25 m	PTI Princeton, NJ
PMT Housing with I/V	PTI MOD 01-512	PTI Princeton, NJ
PMT	R955	Hamamatsu Corp. Bridgewater, NJ
Nebulizer	Concentric TR-50-C2	J.C. Meinhard Santa Ana, CA
Spray Chamber	Scott	Laboratory Built
Lens	f/3, suprasil	Oriel Corp. Stratford, CT
Rotameters	MM3	Air Products
Column	Delta Bond 10 cm x 1 mm 5 um particles	Keystone Sci. Pittsburgh, PA
Pump	SFC/200A	Suprex Corp. Pittsburgh, PA
Oven	Single Wall Transite	Blue M Electric Co.

and converted to voltage via a PTI MOD 01-512 model current-to-voltage converter. Then the resulting voltage was sent to a strip chart recorder.

Two different geometries of viewing were employed for collection of data with the SFC-HEMIP system, Figure 8 and Figure 9. Studies employing argon as the plasma gas were conducted in the radial mode, unless otherwise stated. Experiments with helium as the plasma gas were carried out in the axial mode.

Minimal Detectable Quantity

The term minimal detectable quantity (MDQ) is related to the smallest detectable sample that can be read above the noise level at an 80 percent confidence level. For chromatography it has been almost universally, yet arbitrarity, decided that the smallest readable response above noise should be a factor of two. One method [35] of calculating the MDQ is defined by dividing the sensitivity into twice the noise level. The equation for calculating the MDQ is as follows:

$$MDQ = 2*N/S$$

where N is the noise level and S is the sensitivity.

Limit of Detection

The limit of detection (LOD) is related to the smallest detectable sample that can be read above the noise level at a 95 percent confidence limit. This method (unlike the MDQ) has been sanctioned by IUPAC and is calculated using the following equation [36]:

$$c_L = (k*s_{bk})/m$$

where c_L is the limit of detection, k is the confidence value, s_{bk} is the standard deviation of the background, and m is the analytical sensitivity. The k value used for all calculations was two, rather than three. This lower k value was used only for comparative purposes with the existing literature.

Data Collection

For diagnostic studies (electron number densities and excitation temperatures) in the axial or radial mode, the plasma was translated in the X- and Y- direction via translation stages (NRC) to yield the optimum observation zone. Each data point represents the average of a least ten observations. It should be noted that the studies were resolution limited (0.25 m monochromator with resolution of 1.2 A using 20 um slits) and the calculated electron densities and excitation temperatures were used for this

work only for relative comparsions of CO_2 flow rates on the plasma.

The chromatograms were collected at a fixed position (0.5 mm above the cavity face) in the radial mode and slightly off center for the axial mode. The radial mode allowed improved selectivity [37] due to a more stable plasma viewing zone, while the axial mode allowed greater sensitivity. The sample chromatograms were collected with the use of a strip chart recorder.

Chapter 3

DIAGNOSTIC MEASUREMENTS OF THE ARGON-HEMIP

The understanding of the physical parameters involved plays an important role in the development of any atomization source for spectrometric analysis. This understanding provides the information necessary for the determination of plasma properties such as excitation temperature and electron number density. In addition, this understanding can be used as a basis for describing fundamental mechanisms or processes which relate the interactions between analyte species (atoms, ions, and molecules) and plasma species (electrons, atoms, ions, and molecules).

In fundamental theory, a temperature may only be defined for systems in thermodynamic equilibrium, TE. For the latter to exist, several criteria must be fulfilled [38]:

a.) The velocity distribution function of all particles must follow the Maxwell equations.

b.) The excited states must be populated according to the Boltzmann distribution.

c.) The distribution of molecules and their dissociation products must behave according to the mass action law of Guldberg and Wagge.

d.) The distribution of the atom-ion equilibria must follow the Saha-Eggert relationship.

e.) The distribution of the electromagnetic radiation in the plasma must be in agreement with Planck's law.

Hence, a system is only in TE if it can be described by a single temperature. That is, the electron, gas, excitation, and ionization temperatures must be equal.

Unfortunately, no laboratory plasma exists in a state of TE. Despite the deviation from TE, the useful concept of local thermal equilibrium (LTE) can be employed [39]. A system is said to be in thermal equilibrium when the distribution of the velocity of the particles and the population of their energy levels can be described by a single value of a temperature. This concept can be extended for situations where thermal equilibrium is established at each point in the plasma but allowing for the possibility of different temperatures at different points. Thus, one may speak of LTE characterized by local temperatures. The state of LTE is reached when the rate at which the energy is equally partitioned over the different degrees of freedom is much faster than the rate of transport of heat and mass through the plasma. Therefore, laboratory plasmas and flames are described qualitatively and quantitatively in terms of their deviation from LTE.

In order to evaluate the effects of carbon dioxide on the plasma's physical parameters, the most important

criteria are temperature and electron number density measurements. These values will give insight in to the extent of departure from LTE, and are extremely helpful in making educated predictions with respect to atomic emission signals.

In this chapter, diagnostic studies of the Ar-HEMIP are presented. Diagnostic measurements include excitation temperatures, electron number densities, plasma geometry, and the effects of CO_2 on atomic emission signals.

EXPERIMENTAL

The following experimental information is in addition to the information in Chapter 2. The Ar-HEMIP was viewed in the radial mode for all measurements reported in this chapter, unless otherwise stated. A 50 um slit width was employed. A 1.0 mm circular aperture was mounted in front of the entrance slits of the monochromator upon which the plasma radiation from the Ar-HEMIP was focused. The plasma was translated in the X and Y direction via translation stages (NRC).

Data sets for excitation temperature and electron number density studies represent an average of at least five repeated experiments. All reported data are background corrected.

Excitation Temperature

The excitation temperature of the Ar-HEMIP was determined from the spectral emission intensities of an iron stock solution [39]. An iron stock solution of 1000 ppm was introduced into the plasma and the relative intensities of the iron atom lines (373.2 nm and 374.9 nm) were measured. The excitation temperature was determined using the following equation [40]:

$$T = \frac{(E_1 - E_2)/2.303k}{\log(A_1\, g_1\, \lambda_2/A_2\, g_2\, \lambda_1) - \log(I_2/I_1)}$$

where E= excitation temperature
A= transition probability
g= statistical weight
λ= wavelength
k= Boltzmann constant (6.24×10^{18} eV/K)

and the subscripts 1 and 2 refer to two lines in the iron spectrum. Constants for the two-line method calculation are listed in Table 3.

Electron Number Density

The electron number density determinations for the Ar-HEMIP were done employing the method of Stark broadening [38]. Atomic hydrogen lines are most frequently used for this determination because of the availability of extensive tabulations of Stark broadening parameters for the complete line profiles [41-43].

Table 3: Wavelengths and Constants Used in Excitation Temperature Measurements

Wavelength (nm)	g*A (1/s)	Excitation T (eV)
372.2	4.60 E+7	3.416
374.9	6.40 E+7	3.416

The determination of the electron number density by full-width at half height (FWHH) of the hydrogen-beta Balmer line (481.1 nm) was employed for several advantages [38]:

a.) it is relatively free from spectral interferences by plasma components.

b.) the range of FWHH anticipated (approximately 1.0-5.0 A) and the relative intensities observed were sufficiently large to allow accurate measurements at various observation heights in the plasma.

c.) extensive Stark data were available for complete line profiles encompassing a broad range of electron number density values and temperatures.

d.) greater accuracy is generally associated with Stark calculations for the hydrogen-beta line than for other atomic hydrogen lines.

The electron number density can be calculated from the FWHH by the following equation [38]:

$$n_e = c(n_e, T)(\lambda_s)^{3/2}$$

where $c(n_e, T)$ is a function of electron density and temperature,

λ_s is the FWHH of the hydrogen-beta line. $c(n_e, T)$ values are tabulated in Griem's book [42] for different values of electron temperature and electron number density.

RESULTS AND DISCUSSION

Effects of CO_2 on Excitation Temperature

Although the exact effect(s) of carbon species on atomic spectrometric signals is not completely resolved among atomic spectroscopists, it has been noted that the combustion and decomposition products of carbon containing species absorb plasma energy [44, 45] resulting in diminished atomic emission signals of the analyte. This effect of energy absorption on plasma temperature can be seen in Table 4, where the excitation temperature decreases as the flow rate of CO_2 increases.

This observation suggests that the performance of the MIP is reduced with the introduction of CO_2. This is not surprising, since organic nebulization into the inductively coupled plasma (ICP) shows similar results. The decrease in the excitation temperature, for the MIP and ICP, by introduction of organic species into the plasma source can be attributed to the absorption of energy by molecular species (CO, C_2, CN, etc.) from the plasma. According to Blades [44], the molecular carbon species absorb energy from the plasma source and affects the thermal conductivity of the plasma during the process of dissociation. This lowering of the excitation temperature of the Ar-HEMIP with

Table 4: Effect of Carbon Dioxide on T(exc)

Carbon Dioxide Flow, (mL/min)	T(exc), (K)
0	3300(± 3%)
5	3100(± 3%)
10	2400(± 3%)

the introduction of CO_2 is similar to that of a 1.75 KW ICP, where a reduction in the excitation temperature by the nebulization of organics was found to be approximately 1500 K [44].

Effects of CO_2 on Electron Number Density

Table 5 shows the electron number density, n_e, as a function of CO_2 flow rate as determined by the full-width at half height from the broadening from the hydrogen-beta line at 486.1 nm. Due to the limited resolution of the monochromator employed these determinations are for comparison of relative change within this study. However, these relative values are useful in illustrating an n_e trend with increasing mass flow of CO_2 into the plasma. The trend for this study shows an initial decrease in the n_e with the introduction of CO_2 but is followed by a leveling off.

Plasma Geometry

The shape of the plasma discharge appears to be symmetric, but a lateral profile of calcium emission at a fixed height suggest that the plasma is actually asymmetric, see Figure 10. This asymmetry may be accounted for by a non-uniform flow pattern of the laboratory constructed torch. The maxima are found to be at -1.5 mm and +2.0 mm

Table 5: Effect of Carbon Dioxide on Electron Number Density

Carbon Dioxide Flow, (mL/min)	Ne-, (e-/cc)
0	1.3 E+15(+ 4%)
5	2.1 E+14(± 4%)
20	2.1 E+14(± 4%)

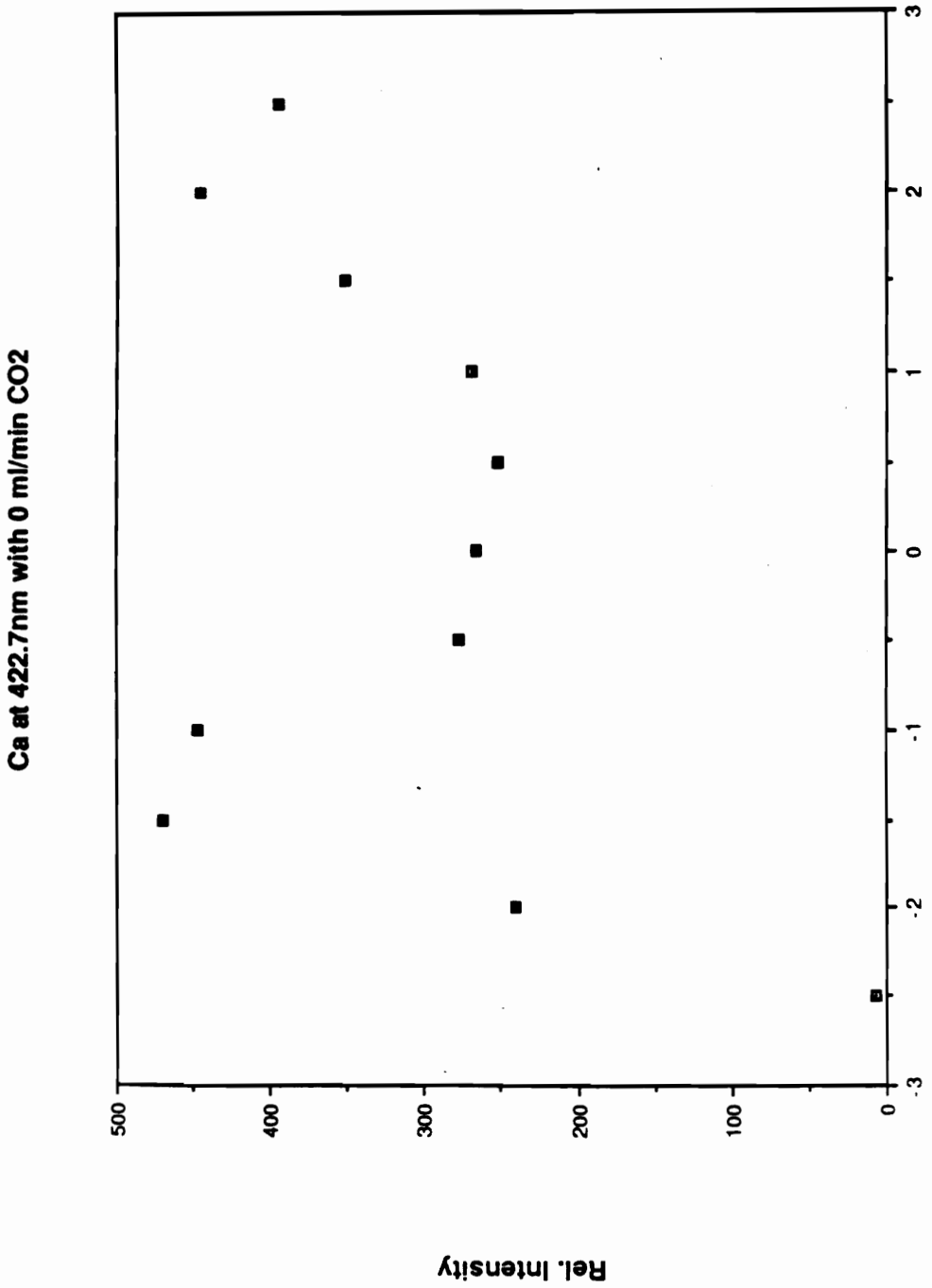

Figure 10: Lateral Profile of the Radial Mode for Calcium Emission with 0 mL/min CO_2

from the center of the torch. Therefore, the location of the maximum atomic emission signal may vary from one torch to another.

Effects of CO_2 on Plasma Geometry and Analyte Signal

The introduction of CO_2 into the plasma has been shown to affect the excitation temperature and the electron number density, Table 4 and Table 5, respectively. In addition, it can be seen in Figures 11-13 that the location of the maximum emission signal has shifted to -0.5 mm and +1.5 mm with the addition of CO_2, when compared to the profile with no CO_2 added, Figure 10. Also, there is a continual decrease in analyte signal across the profile as the flow rate of CO_2 is increased.

Effect of CO_2 on the Maximum Atomic Emission Signals

In order to characterize the effect of CO_2 on atomic emission signals aqueous calcium, chromium and cobalt were chosen as test elements. It has been previously shown [25] with supercritical fluid CO_2 sample introduction into an ICP that Ca(I) emission decreases with increasing amounts of CO_2. Olesik proposed this observation could be contributed to the formation of molecular species such as CN. This hypothesis was also confirmed by Long and Bolton [44]. In Table 6, the analyte maximum emission signals show the same

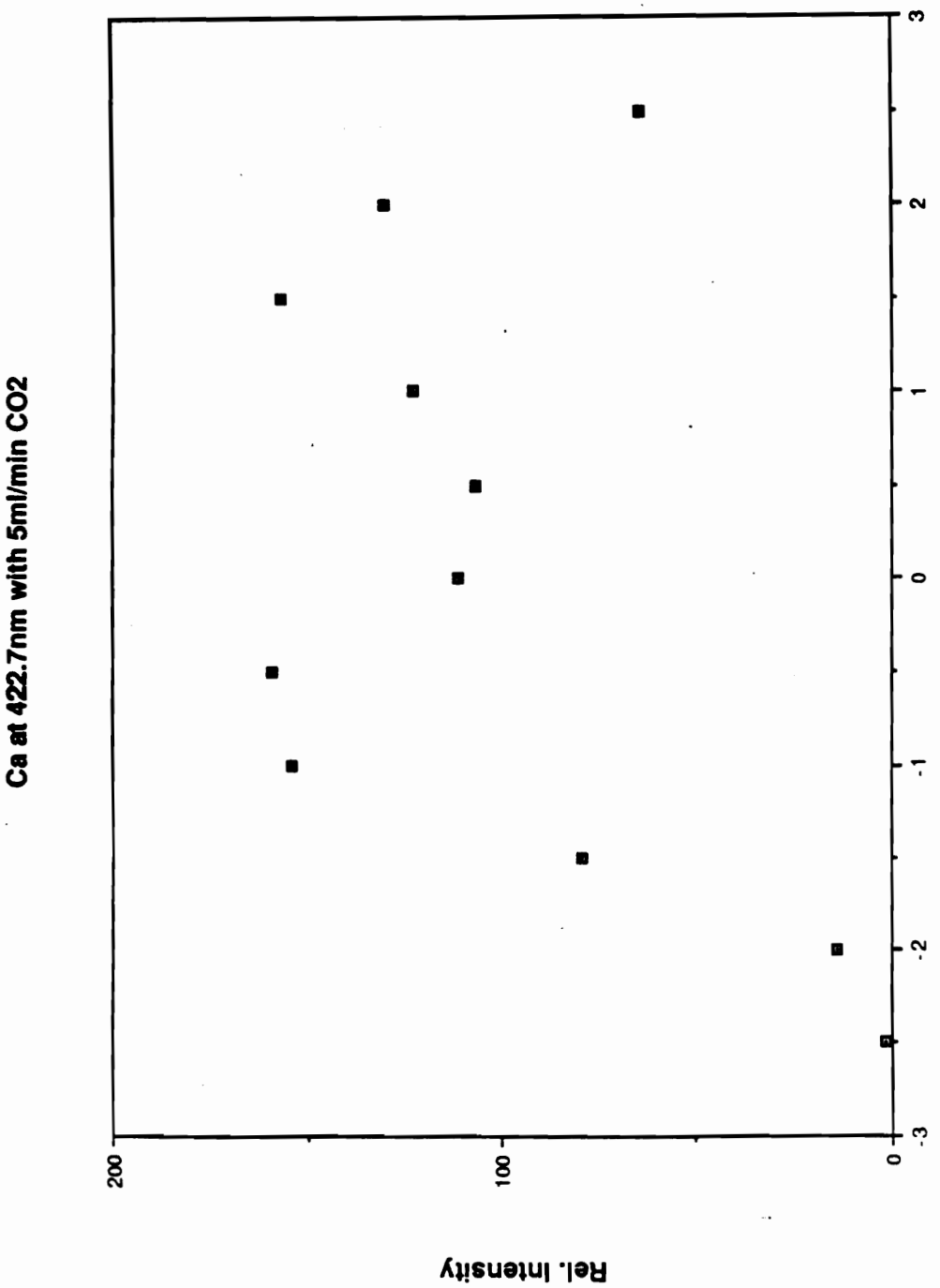

Figure 11: Lateral Profile of the Radial Mode for Calcium Emission with 5 mL/min CO_2

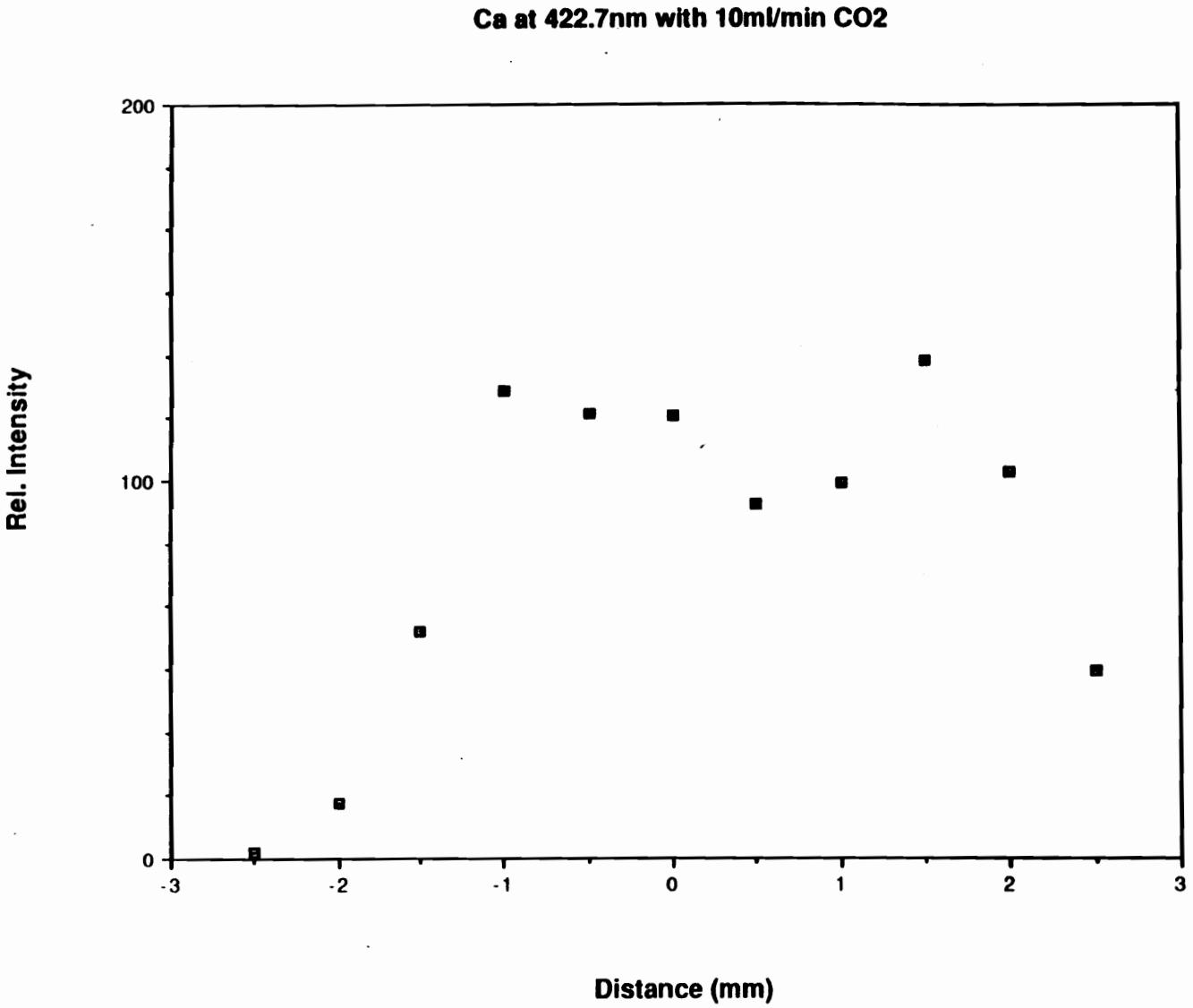

Figure 12: Lateral Profile of the Radial Mode for Calcium Emission with 10 mL/min CO_2

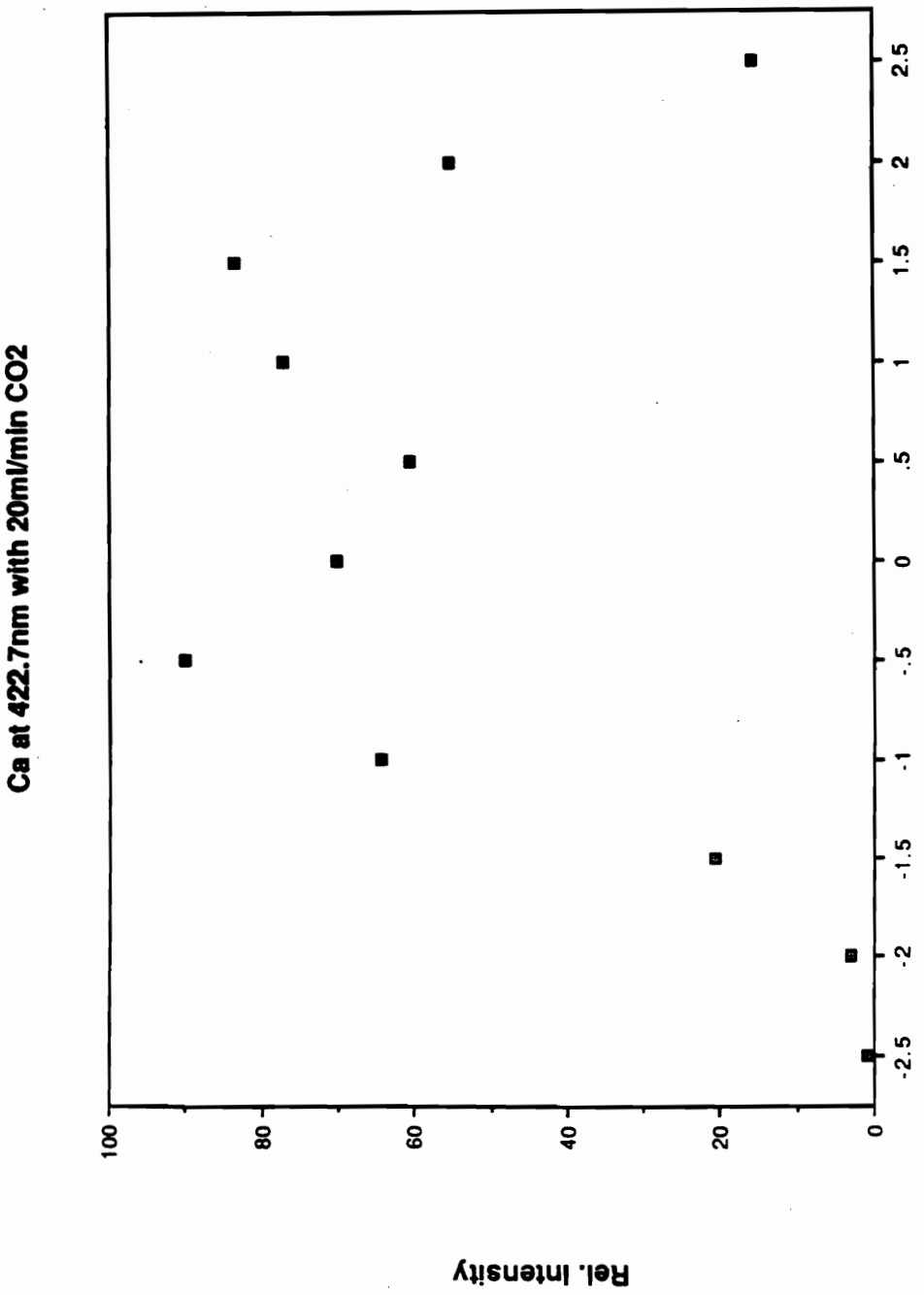

Figure 13: Lateral Profile of the Radial Mode for Calcium with 20 mL/min CO_2

Table 6: Effect of Carbon Dioxide on Atomic Emission Signal in mV

Carbon Dioxide (mL/min)	Ca(I)	Cr(I)	Co(I)
0	490	191	118
10	160	156	72
20	40	80	38

results, not only for Ca(I) but also Cr(I) and Co(I), indicating that carbon species have a direct effect on plasma energy, thus on analyte emission signals.

SUMMARY

The high efficiency microwave induced plasma is affected by the introduction of CO_2. However, the performance of the HEMIP with the CO_2 model studies showed sufficient promise to continue with the supercritical fluid chromatography experiments.

The plasma remained ignited over all experimental parameters investigated for the CO_2 model studies. Although, when the amount of CO_2 was increased, the excitation temperature continued to decrease, along with the atomic emission signal. However, the electron number density initially decreased and then leveled off. The introduction of CO_2 caused the location of the maximum atomic emission to shift, when compared to no CO_2 added. Therefore, care must be taken to locate the maximum atomic emission.

Chapter 4

The Evaluation of Sample Introduction Techniques for Packed Column SFC-HEMIP

This chapter will focus on an alternative method for sample introduction that eliminates not only the restrictor freezing but also plasma arcing which will fuse the restrictor tip. The results of central introduction versus sidearm introduction into an argon HEMIP will be discussed. The analytical parameters that will be presented for these different modes of introduction are repeatability, the effect of pressure programming of 100% CO_2 and modified CO_2 on background emission, effects of isobaric pressure on S/N, linear dynamic range (LDR) and the minimum detectable quantity (MDQ) of several organometallic compounds.

EXPERIMENTAL

In addition to the equipment and reagents stated in Chapter 2 the following material was employed. Ferrocene was purchased from Sigma Chemical Company (St. Louis, MO). An industrial sample of dichloro-dimethyl tin was supplied by Suprex Corporation and used without additional purification. The solvent used in the preparation of all samples was HPLC-grade methylene chloride (Fisher Scientific, Raleigh, NC). Methanol and hexanol (both reagent grade) were chosen as the mobile phase modifiers.

RESULTS AND DISCUSSION

Central Introduction

It should be noted that the central introduction required approximately two times the argon flow (see Table 1) over the sidearm introduction in order to maintain a centered plasma over all pressures studied. By using the higher Ar flow for stability when introducing CO_2 into the plasma, a reflected power of 5-10 W was observed, thus indicating a mismatch of cavity and generator. By decreasing the gas flow to 1.8 L/min as with the sidearm configuration, negligible reflected power was obtained.

Pressure Programming

Figure 14 shows the effect of pressure programming (150-350 atm in 10 minutes) for 100% CO_2 and 3% MeOH modified CO_2 at 373.8 nm on the intensity of the background. As noted in previous studies [44, 45], when carbon containing compounds are introduced into an Ar plasma, the background levels in most spectral areas of the plasma rose dramatically . Molecular compounds (C_2, CH, and CO) are thought to give rise to these bands. In the case of pressure programming, in mhich the input of CO_2 into the plasma is not consistent throughout the course of the analytical run, a large change in background levels could

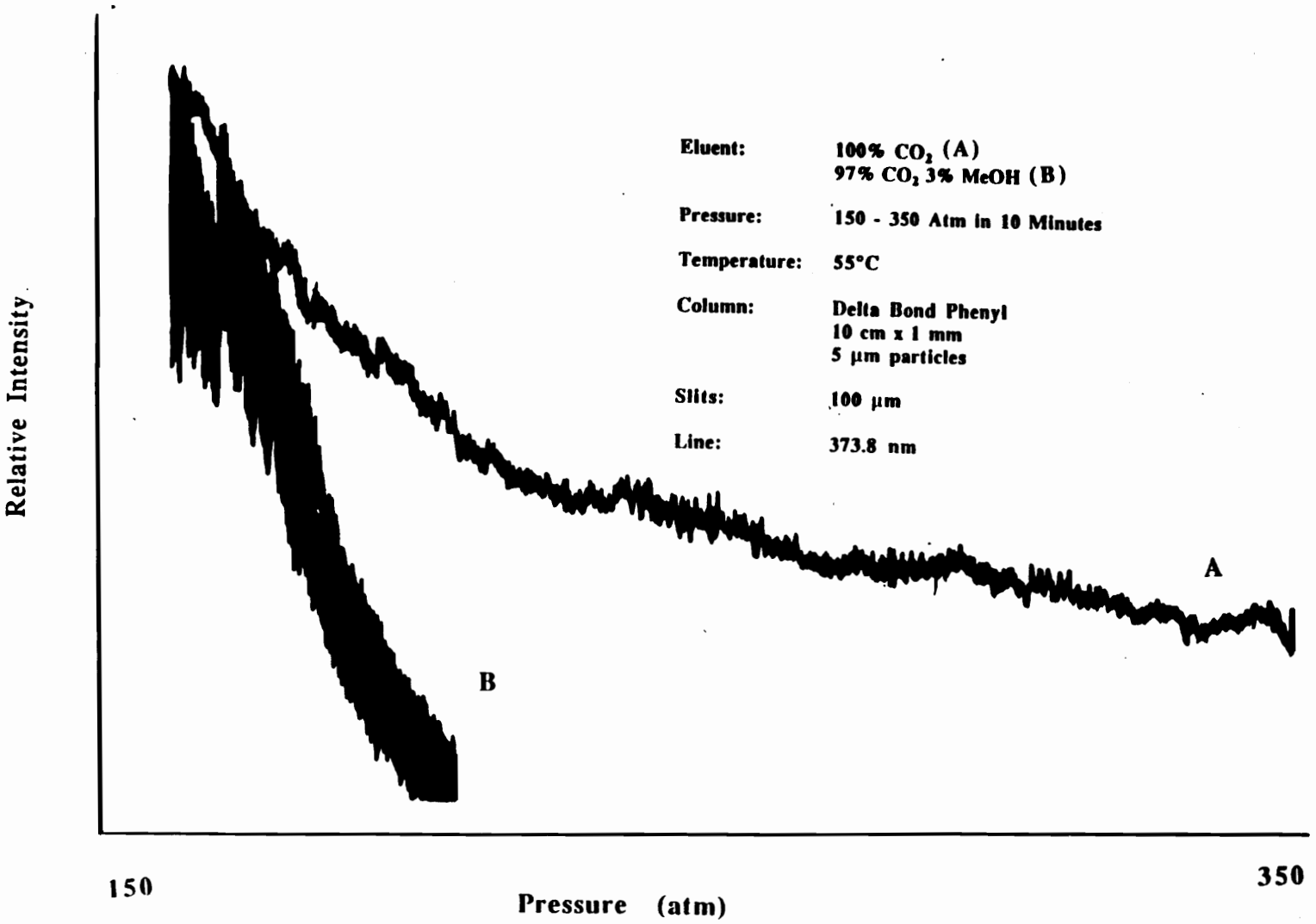

Figure 14: Effect of Pressure Programming on Background Emission Signal without and with Modifier (1 inch= 0.1 V)

diminish the use of a plasma source as an element selective detector for SFC.

To illustrate the background effect, the position of 373.8 nm was monitored using a 2.0 A bandpass for a pressure programming experiment. These data, as illustrated in Figure 14, show the decreasing background from the elemental and molecular gas products of CO_2 as a function of increasing pressure. Additionally, this effect is more dramatic for methanol modified CO_2. This decrease can be attributed to the increased mass flow rate of CO_2 and/or methanol modified CO_2 that is present at higher pressures, thus resulting in the quenching of the excited species in the plasma and an increasing of the reflected power. These same phenomena for CO_2 were noted by Hieftje et al. [24] for SFC surfatron studies, in which a parallel relationship between the baseline slope of the background and the reflected power was observed. They attributed this effect to the detuning of the plasma at higher pressures.

S/N for Fe with Modifier

Figure 15 illustrates the effect of methanol modified CO_2 on the atomic emission signal of Fe in a ferrocene sample. A sample containing 2 ug/uL of Fe and 0.5 uL was injected. One can see in Figure 16 the S/N ratio of a typical sample size injection. The loss of atomic emission

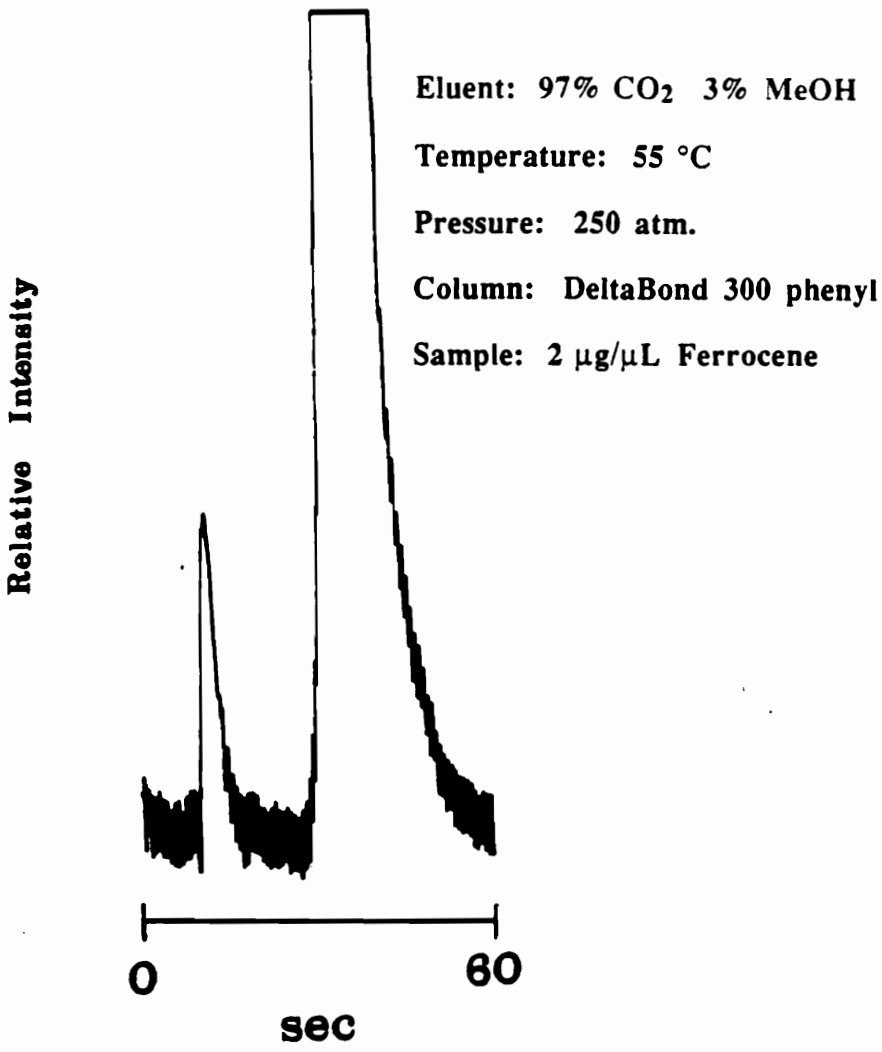

Figure 15: Effect of Modifier on SFC Effluent Atomic Emission Signal (Signal over one volt)

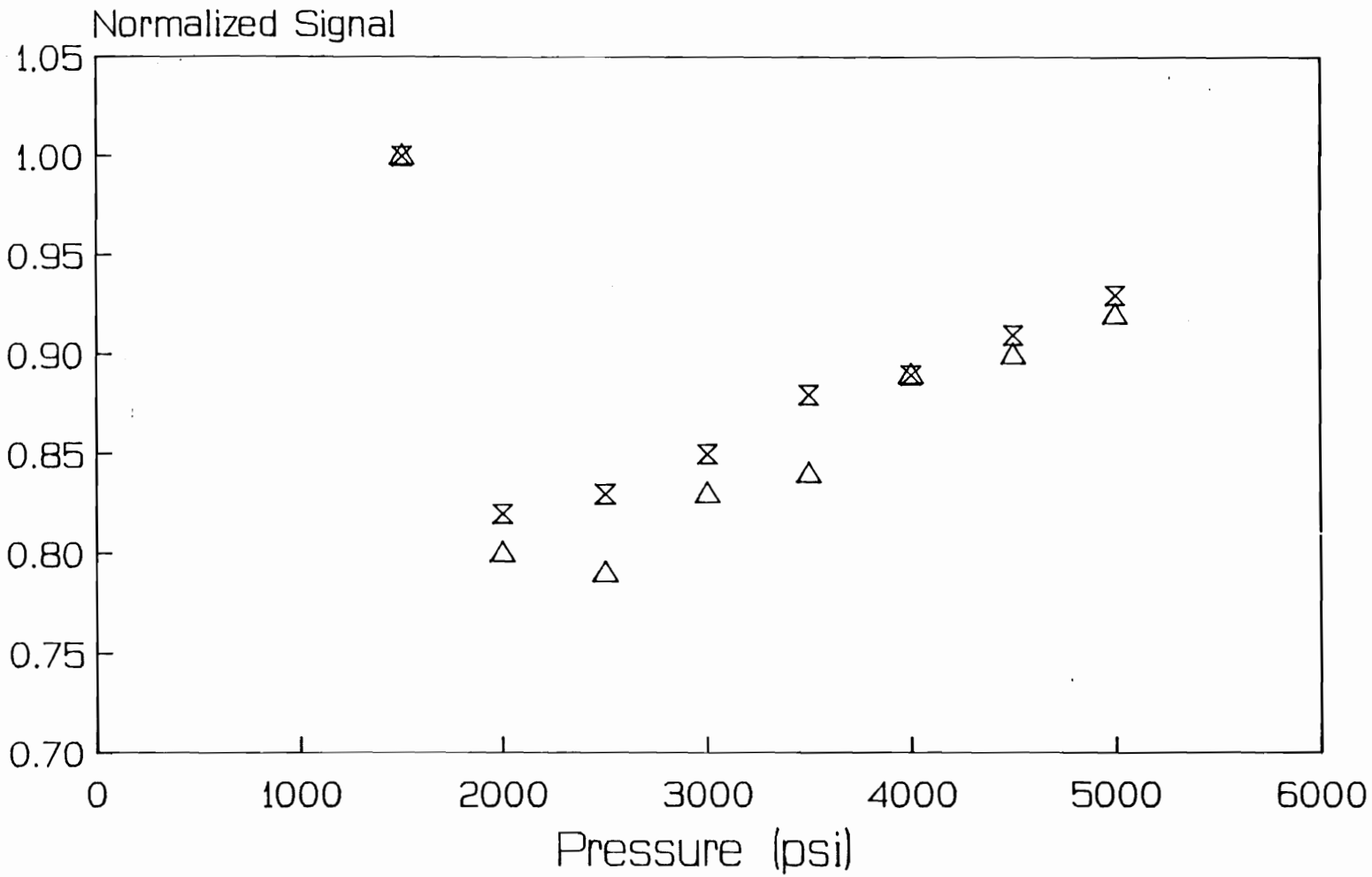

Figure 16: Effect of Isobaric Pressure on Background Emission Signal without and with Modifier

is negligible for a typical sample size injection, even though there is an increase in the noise with the addition of methanol modified CO_2. Therefore, unlike flame-based detectors, the Ar-HEMIP can be employed with 100% CO_2 or modified CO_2.

Effect of CO_2 on Background Emission Signal

It has been noted that the effects of carbon species introduced into an ICP are not easily described [25]. In addition to the plasma being affected, background levels can be affected by broad band emission from the decomposition products of CO_2 (i.e., CN) [37]. Figure 16 illustrates that as the isobaric pressure was increased from 1500 to 5000 psi, the background signal initially deceased followed by a steady increase of the background signal level. The same result was obtained for methanol modified CO_2 but required additional tuning of the cavity. This initial decrease (1500-2000 psi) may partially be explained by plasma instability, whereas, the latter (2000-5000 psi) may be explained by the formation of molecular species (i.e.,CN) as the flow rate of CO_2 is increased.

Sample Chromatograms

The supercritical fluid chromatograms obtained from the atomic emission detection from the HEMIP were not optimized

with respect to experimental parameters such as signal integration, observation height, argon flow rate, mobile phase flow rate or dead volume. Figure 17 illustrates chromatograms that were collected for ferrocene, acetylferrocene and 1,1'-diacetylferrocene with the HEMIP as an element selective detector for Fe. In a previous publication [24], these compounds required 2% MeOH to accomplish sample separation on a conventional phenyl column. It has been noted by Levy [17] that modifiers can be used to increase solubility and decrease column activity resulting in a decrease in retention time, an increase in column efficiency and an increase in column selectivity. In this study, it was experimentally found that these compounds could be separated without the aid of a polar modifier such as methanol. One explanation is that the DeltaBond phenyl packed column is more deactivated than conventional phenyl columns. This improvement in column deactivation reduces sample interaction, retention time and increases column efficiency. This column comparison has also been demonstrated by Taylor and Ashraf-Khorassani [47], in which separations of nitrogen-containing compounds were performed on the DeltaBond cross-linked cyanopropyl bonded phase silica column without the aid of modifiers. Figure 17 shows the HEMIP's response to be ferrocene> acetylferrocene> 1,1'-diacetylferrocene. Employing a UV detector, Taylor et

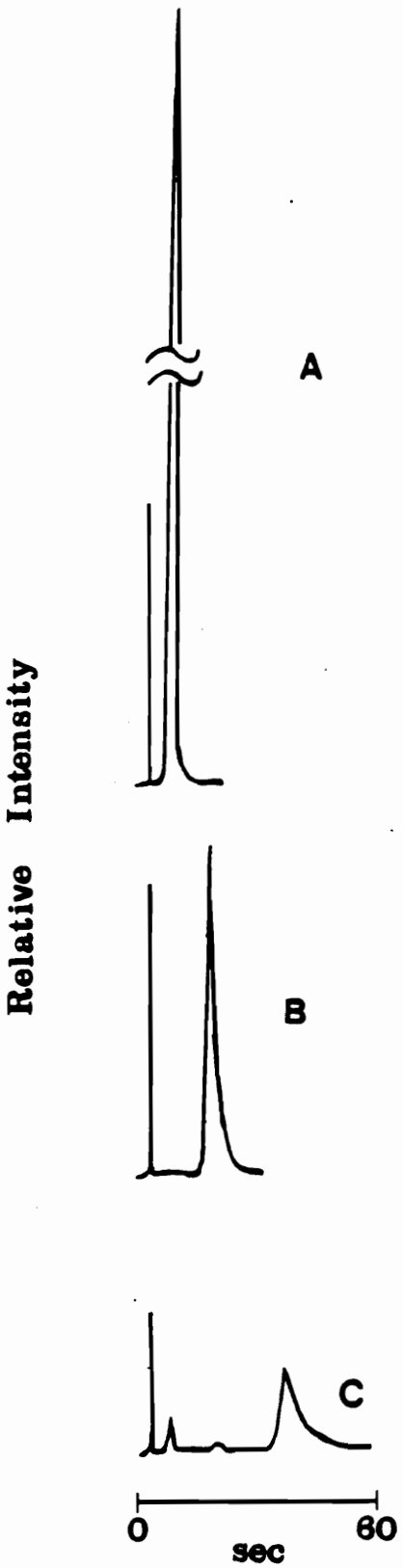

Figure 17: Chromatograms of Single Component Injection of Iron Containing Compounds

al. [24] determined the response to be acetylferrocene> 1,1'-diacetylferrocene> ferrocene. One explanation for the HEMIP's order of response can be attributed to the analyte/stationary phase interaction after noting acetylferrocene has a greater ability to hydrogen bond to the stationary phase than ferrocene and 1,1'-diacetylferrocene has an even greater ability to hydrogen bond than ferrocene or acetylferrocene. This explanation is supported by the broadening of the peaks shown in Figure 17. Therefore this suggests that peak area may be a better means of quantitation rather than peak height, which is routinely employed for atomic emission spectrometry.

An interesting chromatographic feature of the MIP's response is shown in Figure 17C (peaks 1 and 2). Sigma Chemical Company markets 1,1'-diacetylferrocene as 97% pure but without information about the other 3%. One can see in Figure 17A and Figure 17B from the retention times that the 3% is possibly ferrocene and acetylferrocene.

Illustrated in Figure 18 is the chromatogram of ferrocene, acetylferrocene and 1,1'-diacetylferrocene mixture. This mixture contained 2 ug/uL of each compound. This demonstrates the Ar-HEMIP's ability to detect analytes

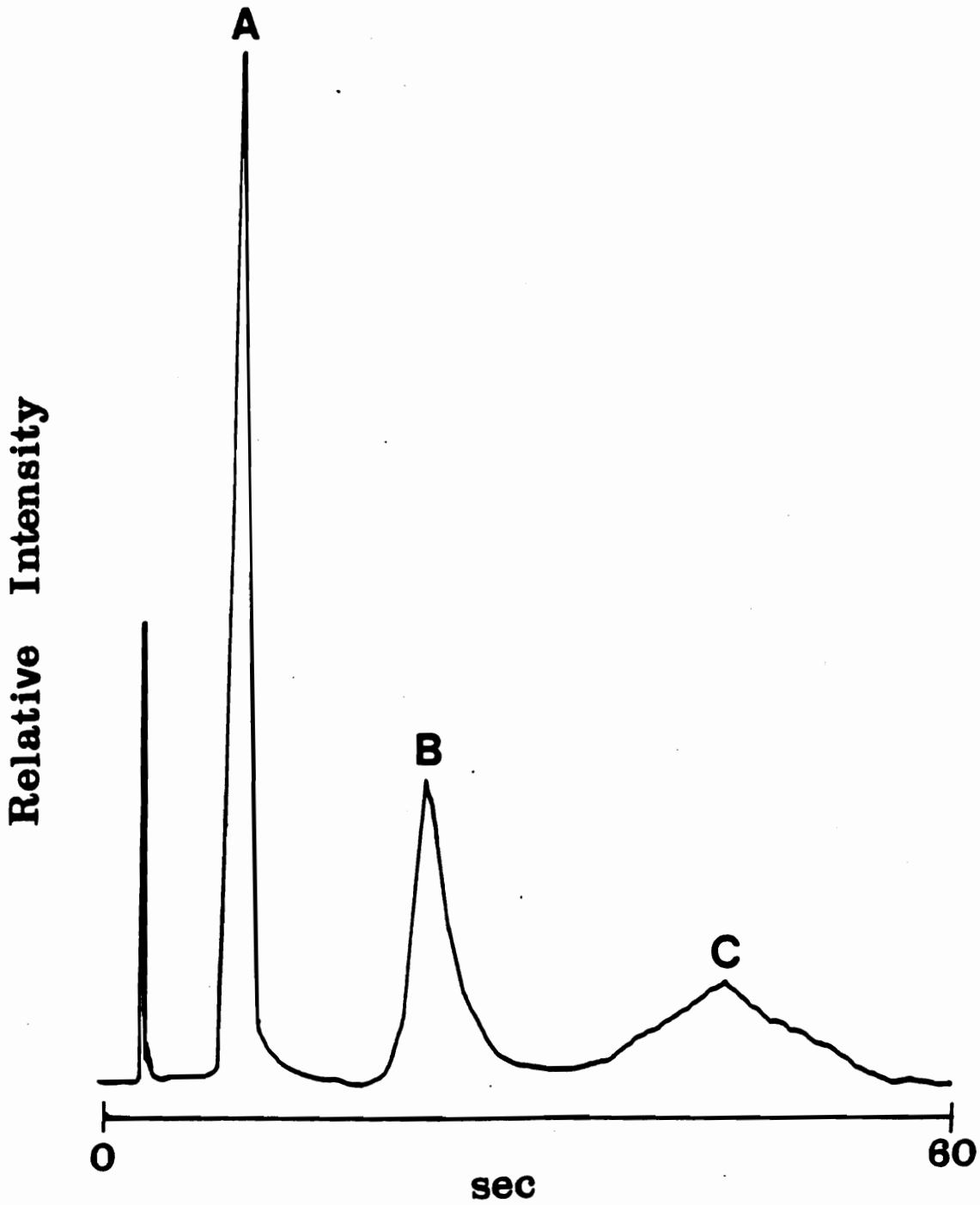

Figure 18: Chromatogram of a Mixture of Iron Containing Compounds

from single component injections or from samples that have multi-element components of interest.

Repeatability

Once the plasma and the restrictor have been made compatible, the system operates quite well, as indicated in a series of repetitive injections shown in Figure 19. This figure illustrates the injection-to-injection repeatability with four replicated injections of ferrocene. The signal is the mV output of the Fe(I) emission line as observed by the spectrometer. The relative standard deviation, RSD, for this configuration has been calculated to be 3 % for concentrations ranging from 0.01 to 2.0 ug/uL at 0.5 uL injected. Hieftje et al. [24] using a surfatron, Olesik and Olesik [15], and Jinno et al. [16] using the inductively coupled plasma have demonstrated similar injection-to-injection RSD's for various samples.

Minimal Detectable Quantity

The central configuration was employed to obtain a MDQ for iron in a ferrocene sample without the use of the DeltaBond phenyl column. The MDQ was calculated (see Chapter 2) using the guidelines defined by Hartmann [35] for chromatographic detectors. The experimental parameters were 30 um slits (bandpass of 0.96 A), 373.8 nm line and -800 V

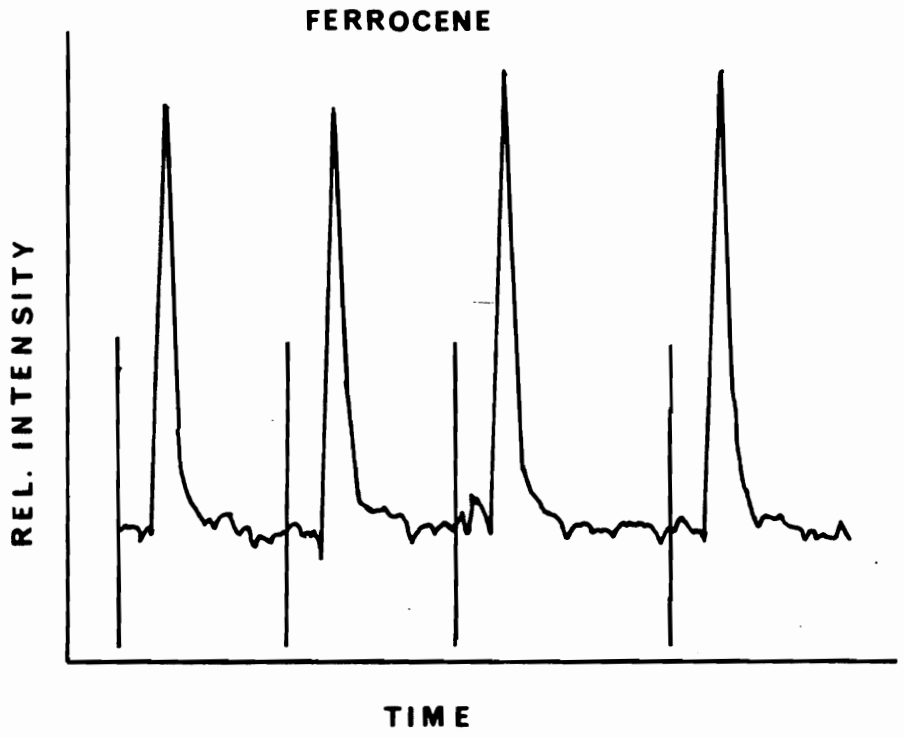

Figure 19: Repeatability of Manual Injection for Central Introduction

on the PMT. The current to voltage converter was operated at 10^{-6} A/V sensitivity. The SFC pressure was held constant at 100 atm at an oven temperature of 110^{0} C. Under these experimental conditions the MDQ for iron was determined to be 0.03 ng. It should be realized that this value for the MDQ is the minimum quantity of sample the detector should be able to measure assuming a perfect separation with the only noise in the measurement coming from the detector and no random noise associated with the separation. In reality this chromatographic MDQ is much lower than what could be defined as the limit of detection for the system. Using the IUPAC [48] definition of 20 background readings, and k=2 instead of k=3, a C_L of 20 ng is calculated. This value which reflects the total noise that a system would monitor is a better measure of the detection limit than the MDQ. However, because most chromatographers report the MDQ measurement based on the detector noise, the MDQ will be reported as 0.03 ng. However, the sidearm configuration offered better signal sensitivity as will be demonstrated later in this chapter.

Sidearm Introduction

Experiments carried out in this mode required the restrictor to be placed in the sidearm of the torch, where the effluent was premixed with the plasma gas. This

configuration introduced the argon flow (1.8 L/min) at a right angle to the restrictor tip, which in return prevented nucleation of the CO_2 as it decompressed. This arrangement also prohibited the plasma from arcing back on the restrictor tip, thus eliminating the possibility of the tip being fused. It allowed for a more homogeneous mixing of the plasma gas/SFC effluent, longer residence time, and an increase in sensitivity .

Pressure Programming

Figures 20-23 shows the effect of pressure programming (150-350 atm in 10 min.) for 100% CO_2, methanol modified CO_2, and hexanol modified CO_2 as a function of monochromator slit width. One important trend to observe from these spectra is the increasing background with increasing pressure. This trend is the direct opposite of that found by Hieftje et al. [24], as well as the data from the "central introduction" in this work. One possible explanation for this reversal could be the cavity, which in this study was tuned for the higher pressure (450 atm) and then returned to the lower pressure (150 atm) before starting the ramp. Therefore, as the pressure ramp increased the cavity was going from a "detuned" state at lower pressures to a "tuned" state at higher pressures. As the cavity is brought into "tune", the plasma gains energy

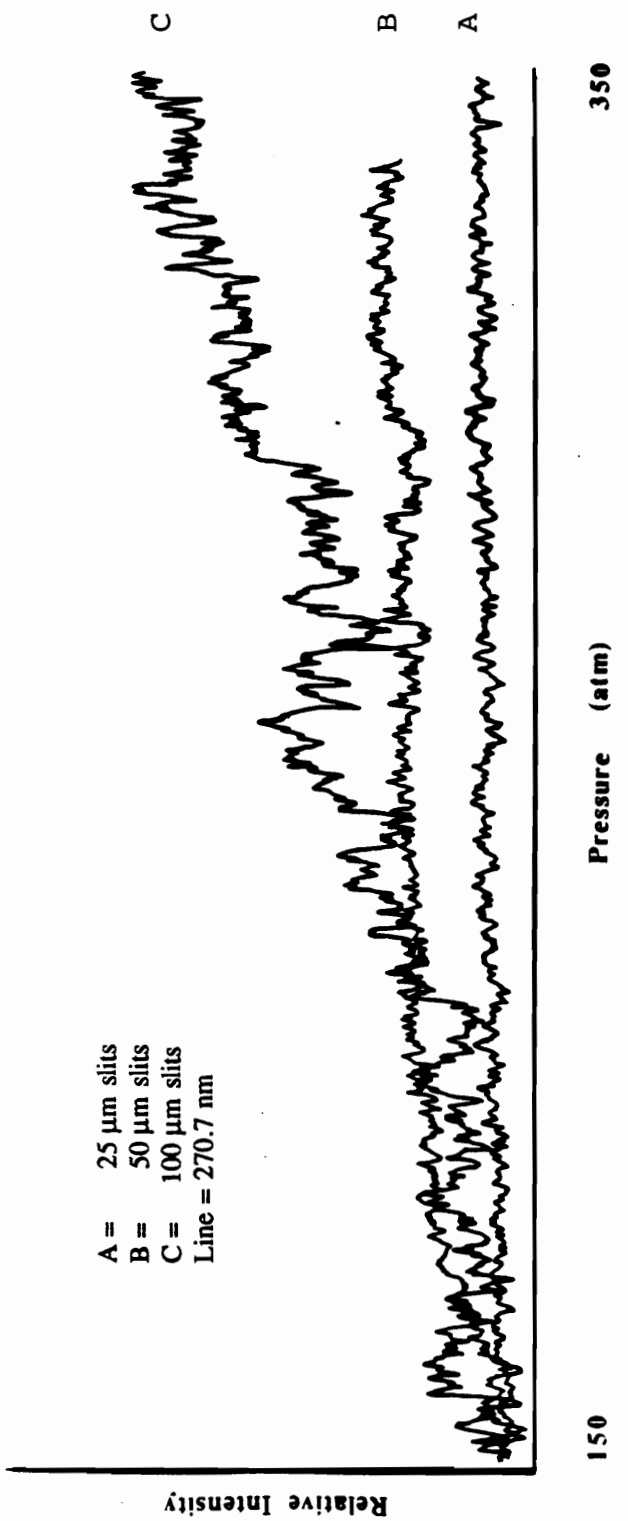

Figure 20: Effect of Pressure Programming with 100% CO_2 as a Function of Monochromator Slit Width (1 inch= 0.16 V)

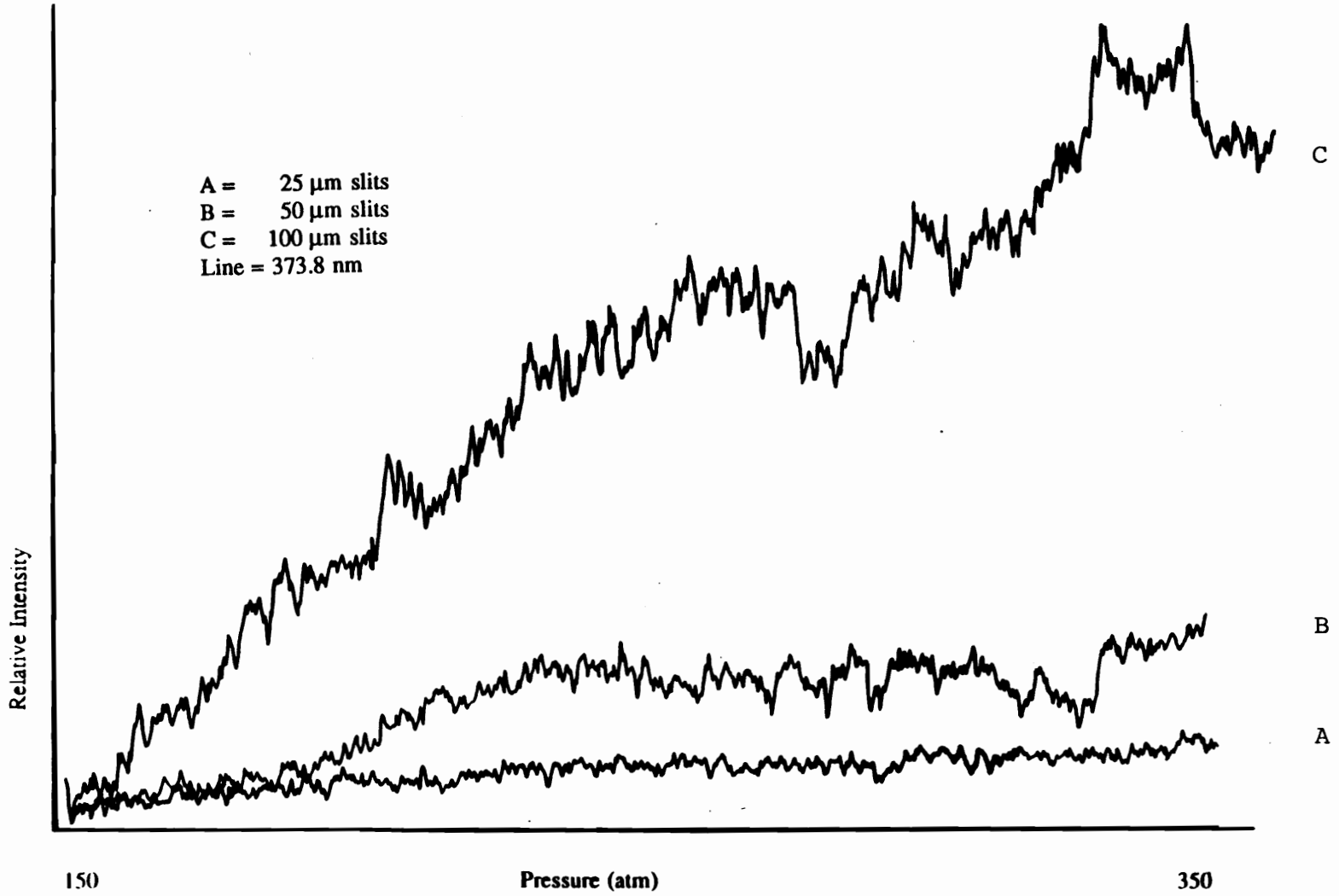

Figure 21: Effect of Pressure Programming with 98% CO_2 2% MeOH as a Function of Monochromator Slit Width (1 inch= 0.15 V)

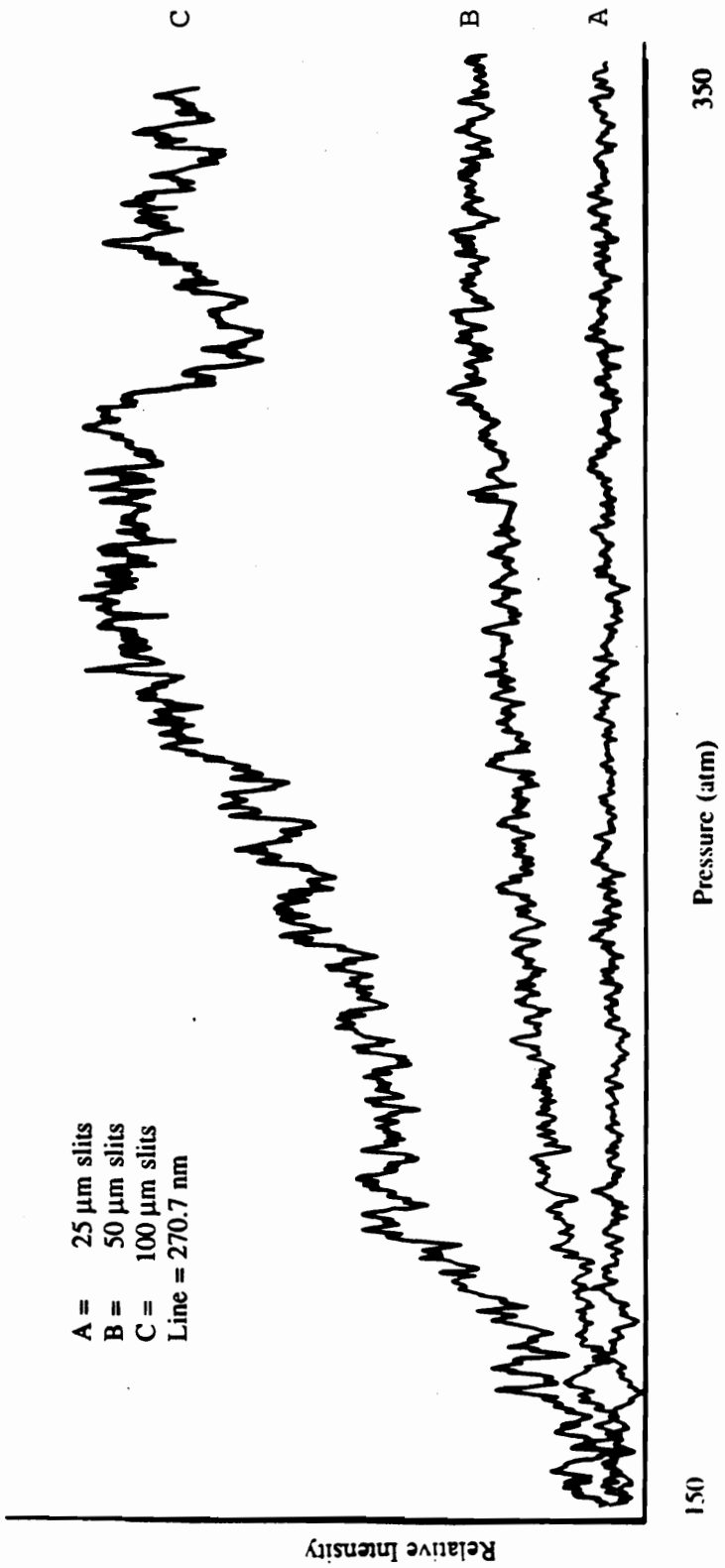

Figure 22: Effect of Pressure Programming with 98% CO_2 2%MeOH as a Function of Monochromator Slit Width (1 inch= 0.14 V)

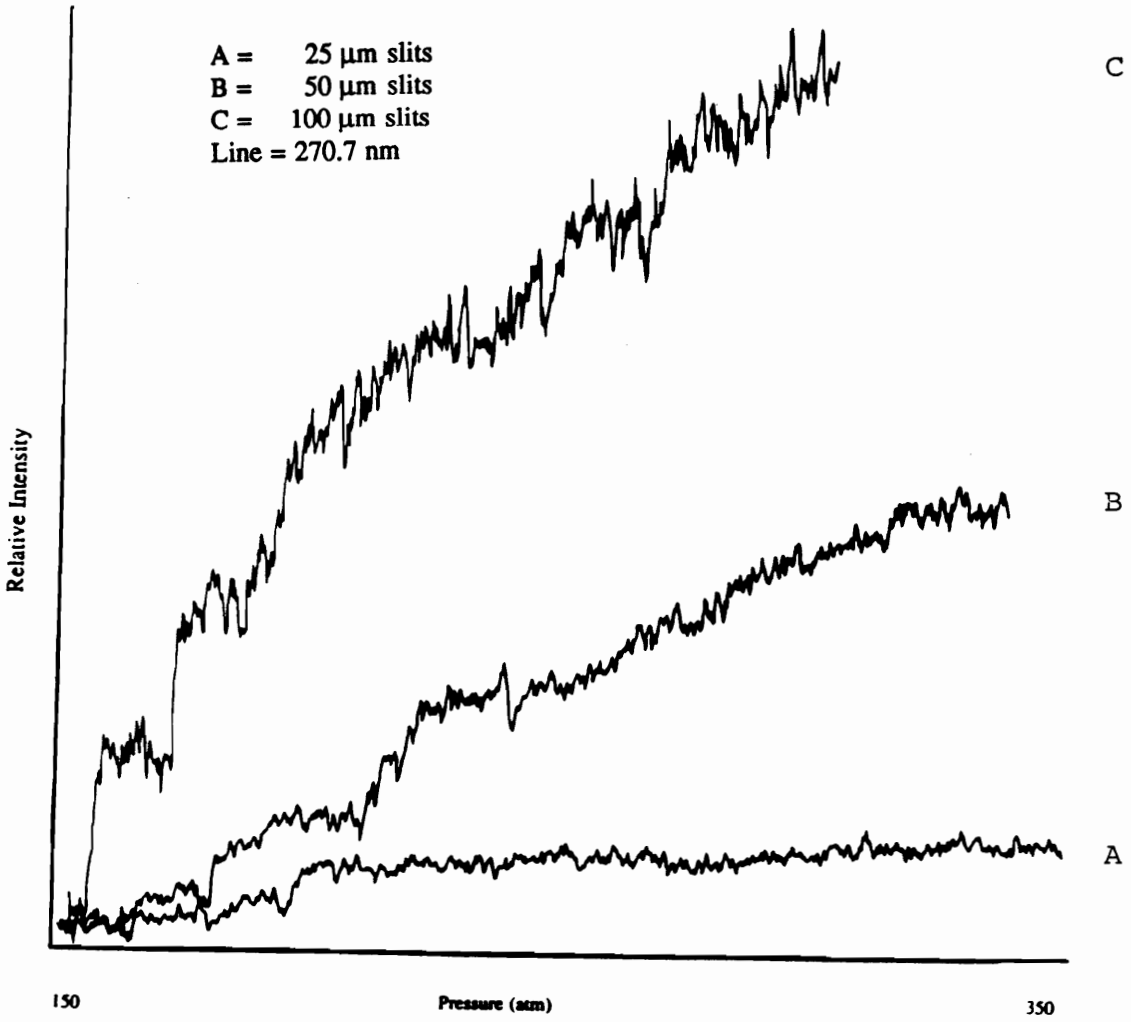

Figure 23: Effect of Pressure Programming with 99% CO_2 1% Hexanol as a Function of Monochromator Slit Width (1 inch= 0.20 V)

and the analyte signal, as well as the background emission increases. The improved sensitivity with the sidearm configuration, in this study, suggests a greater interaction of the analyte with the plasma. Also, this reversal can be supported by the data concerning the argon flow rate decrease with the sidearm configuration, when compared to the central introduction configuration (3.0 L/min to 1.8 L/min, respectively). Additionally, one notices in these figures the increasing slope of the background as the monochromator slit width is increased. This observation suggest that as the bandpass broadens, i.e. as the slit width increases, the emission from molecular species (CO, CN, etc.), which have broader spectral lines, are able to penetrate to the photomultiplier tube thereby increasing the background or noise level.

Molecular Broad Band Emission Species

Figure 24 illustrates molecular species which could be responsible for the increasing background when executing a pressure ramp. These background emission species were identified using references 24 and 49. These species result in broad band emission and cause the background to become more severe as the mass flow of the mobile phase increases with increasing pressure.

Broad Band Molecular Emission Species

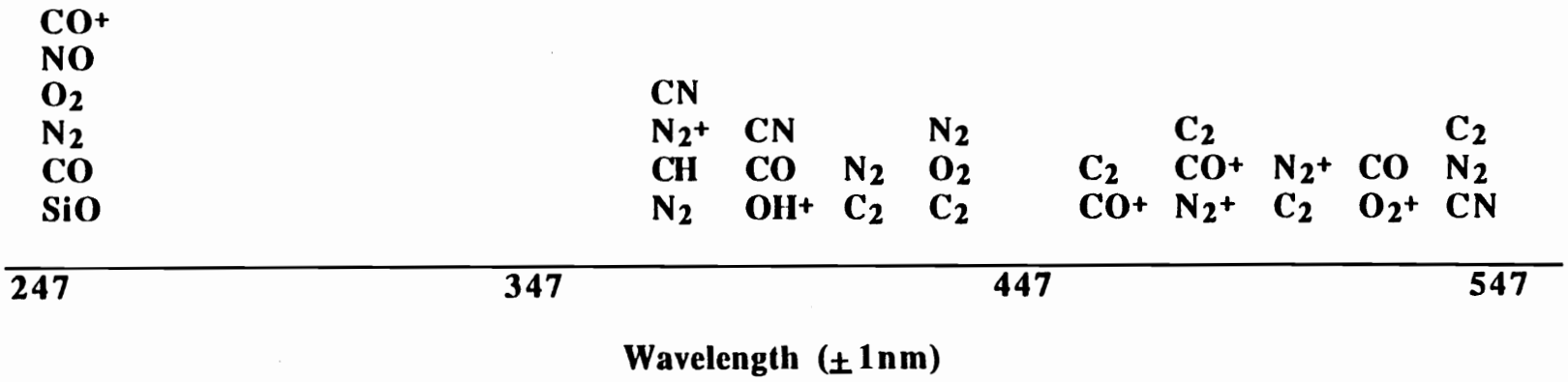

Figure 24: Molecular Broad Band Emission Species

Signal Drift

Figure 25 and Figure 26 illustrate that the emission signal is constant for two isobaric conditions, supporting the background changes shown in Figures 20-23 as a function of increased mass flow rate of CO_2, and not as a result caused by drift. These data were obtained using 2% MeOH modified CO_2 at 150 atm and 350 atm for 10 minutes and at wavelengths 270.78 nm and 373.8 nm, respectively.

S/N Ratios with 100% CO_2 and Modified CO_2

The data in Table 7 were obtained using the DeltaBond phenyl column for comparison of S/N ratios for 100% CO_2 and 1% MeOH modified CO_2. The data for 25 ppm ferrocene at 250 atm and 100% CO_2 gives a S/N=3, whereas for 1% MeOH modified CO_2 the S/N ratio is not regained until 345 atm. The regaining of the sensitivity can be rationalized by an increase in the solvating power of the mobile phase at higher pressures, thus causing the analyte to be more concentrated at the higher pressure by reducing the analyte-stationary phase interaction.

Normalized Signal as a Function of Pressure

The normalized signal of 1000, 500, 100, and 50 ppm Fe from a sample of ferrocene can be seen in Figure 27 as a

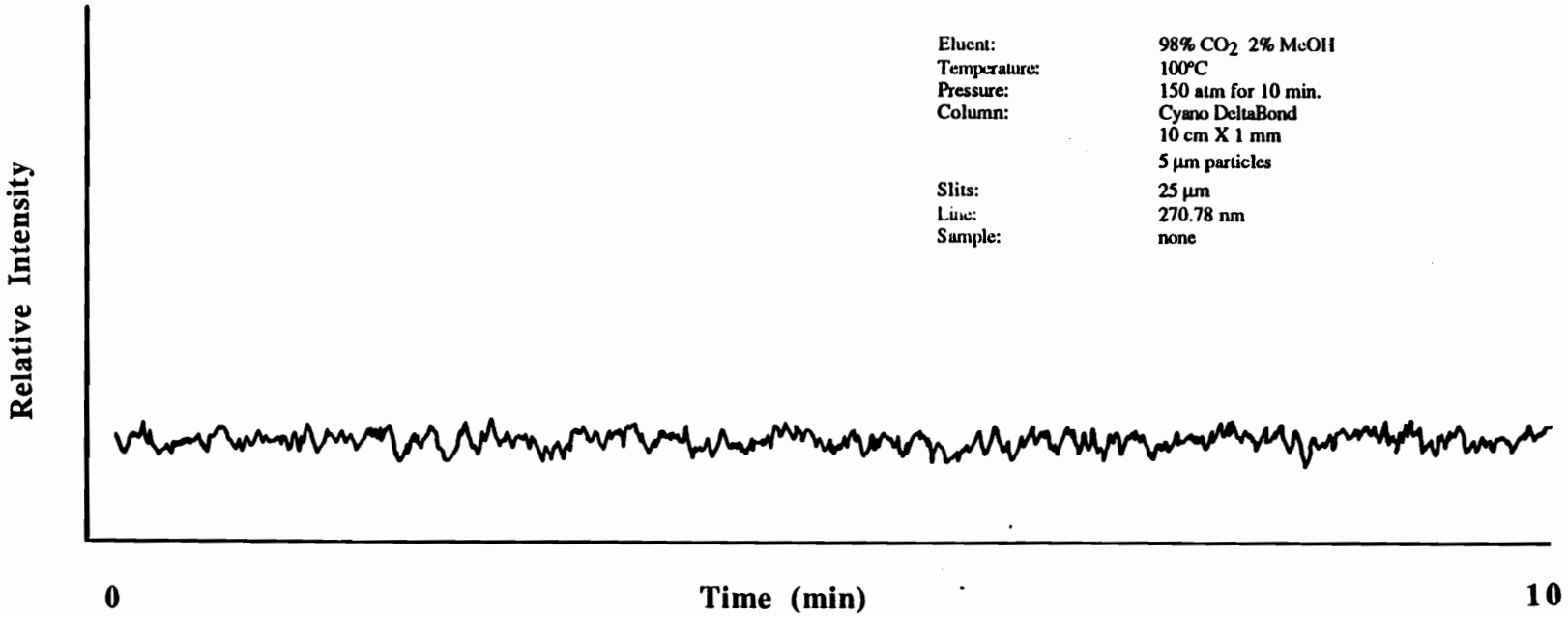

Figure 25: Effect of Isobaric Pressure on Drift (1 inch= 0.1 V)

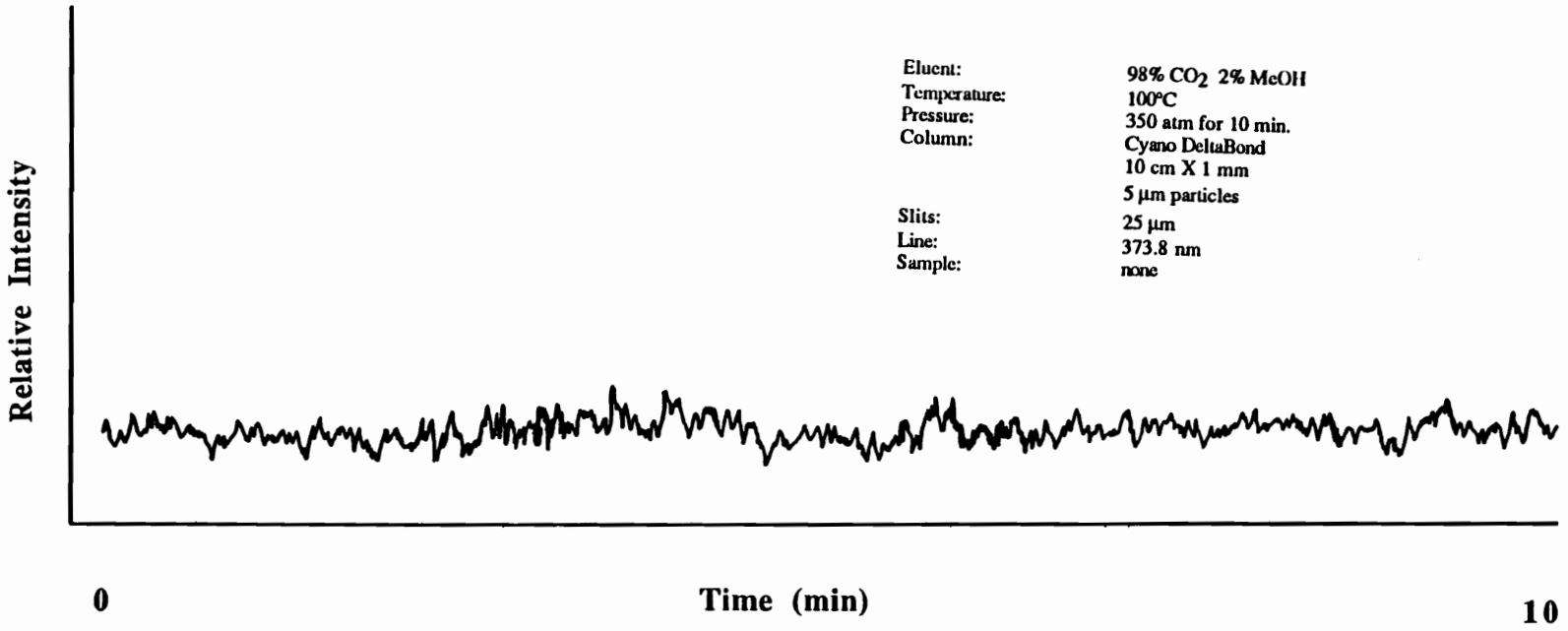

Figure 26: Effect of Isobaric Pressure on Drift (1 inch= 0.1 V)

Table 7: S/N Ratios for 100% CO_2 and Modified CO_2

	S/N for Ferrocene (373.8 nm)			
Pressure (atm)	100% CO_2		99% CO_2 1% MeOH	
	50 ppm	25 ppm	50 ppm	25 ppm
250	5	2.5	3	NS
300	6	3	5.5	2.3
345	6	3	6	3

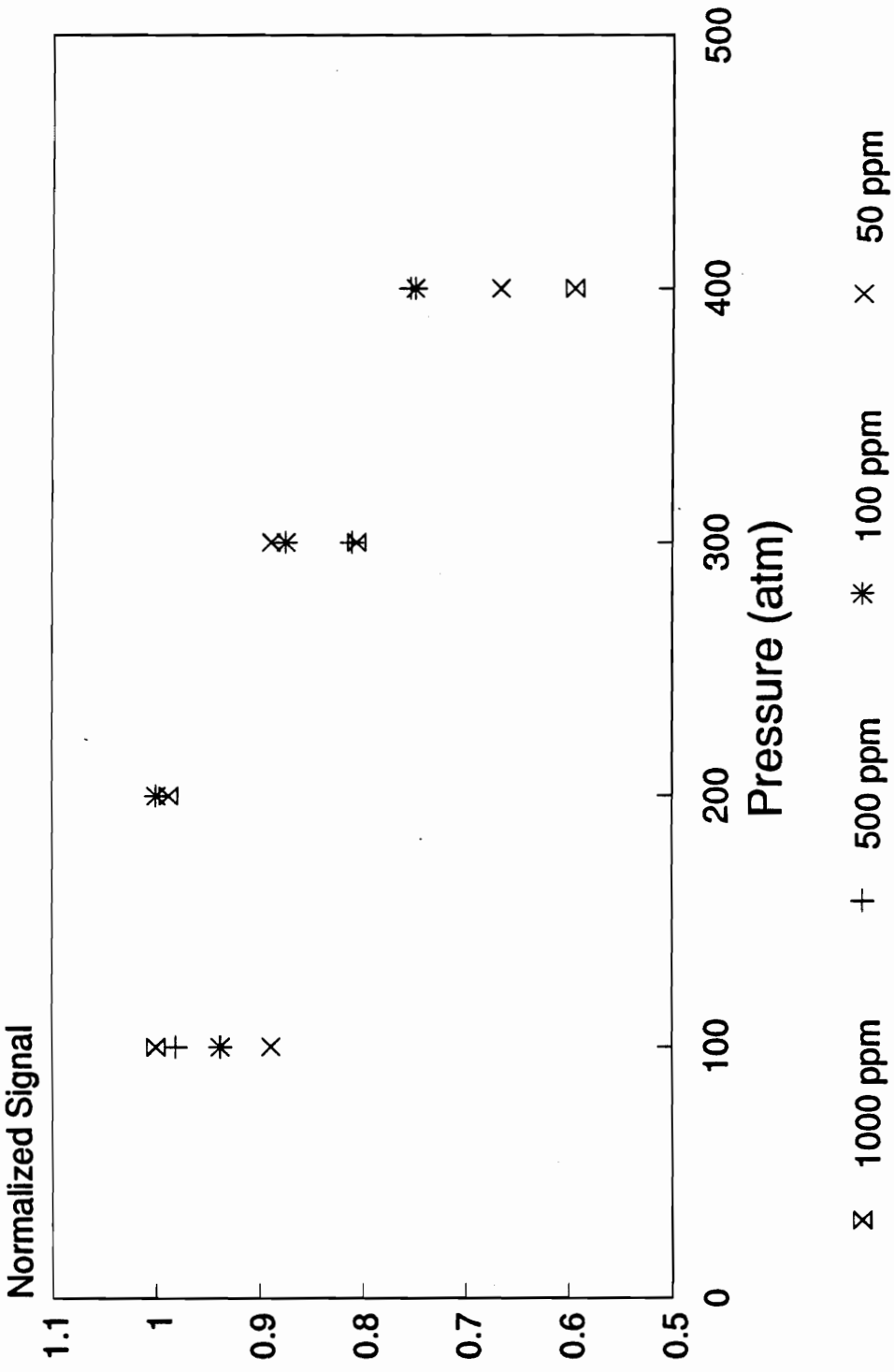

Figure 27: Normalized Signal as a Function of Isobaric Pressure and Analyte Concentration

function of pressure, without retuning the cavity at each pressure. These plots illustrate a decrease in analyte signal with increasing pressure, which suggest an increase in the MDQ when going to higher pressures.

Repeatability

Figure 28 shows four chromatograms that illustrate the repeatability of the sidearm arrangement. The injection-to-injection relative standard deviation was 3%, which is the same as the central introduction. Similar results were reported by authors of references 15, 16 and 24.

Linear Dynamic Range

The mobile phases most commonly used in SFC are molecular fluids. Since the plasma does not differentiate between molecular species, the energy from the plasma is used for decomposition and excitation of both the mobile phase and the analyte. In addition, the increasing mass flow of the mobile phase into the detector as the supercritical fluid is density-programmed absorbs energy from the plasma. These complications are the main reason for the incompatibility of SFC with traditional elemental selective detectors.

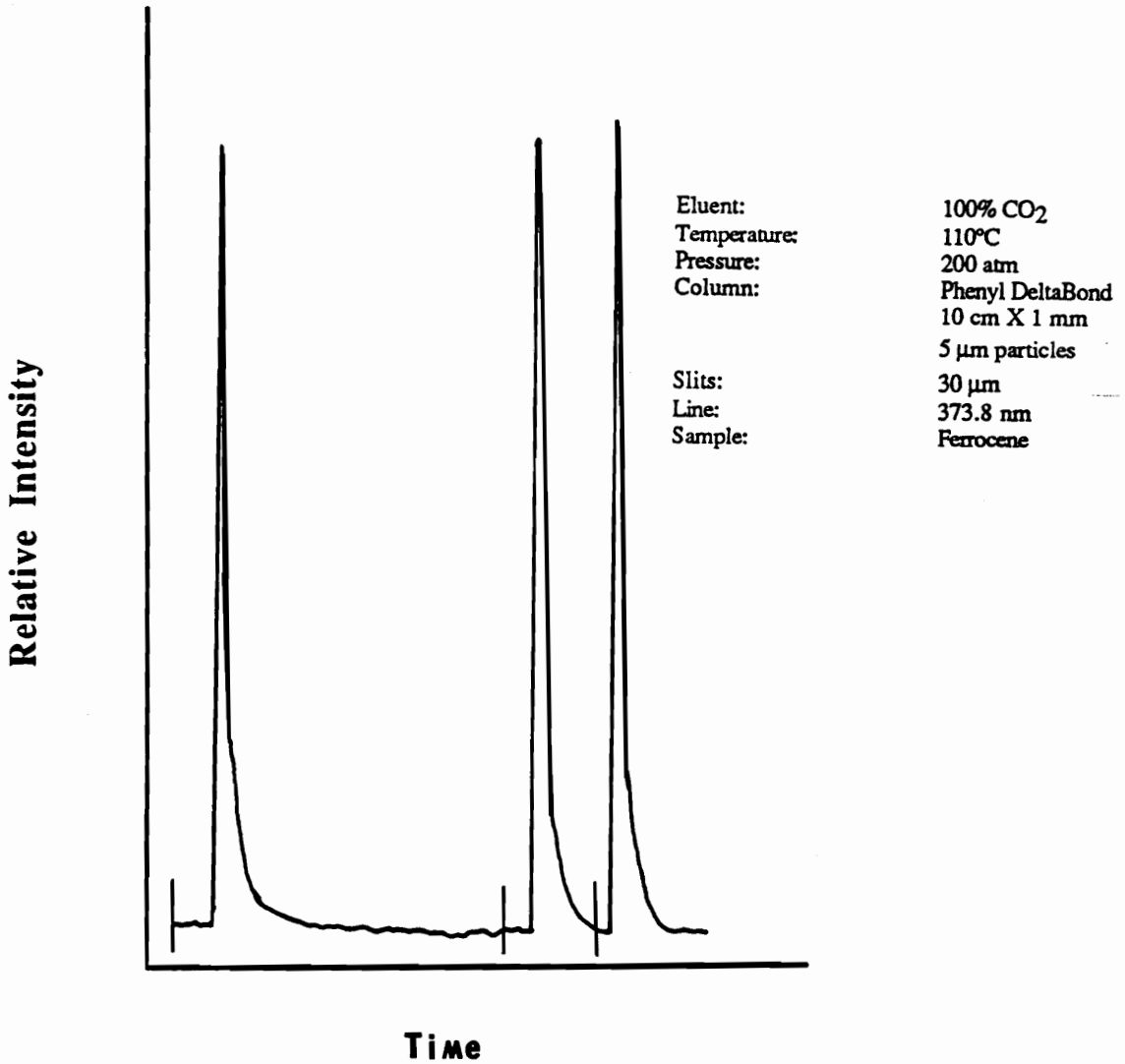

Figure 28: Repeatability of Manual Injection for Sidearm Introduction (1 inch= 0.1 V)

To be of analytical use, the detector must be insensitive to increasing amounts of mobile phase entering the system. This study employing the Ar-HEMIP with the sidearm configuration demonstrates a LDR of at least 2.5 orders of magnitude for Fe in a ferrocene sample (see Figure 29) at pressures of 100, 200, 300 and 400 atmospheres without any statistical difference in the analytical sensitivity. The method of 5% deviation between two consecutive data points for LDR was not employed. Concentrations above one microgram/microliter were not injected, since these samples would be larger than typical sample size for packed columns. Therefore, the LDR for this study is defined as the range from the highest concentration injected to the MDQ. Each of the plots has a correlation coefficient of at least 0.998 for concentrations of 1000, 500, 100 and 50 ppm Fe from a ferrocene sample. This linearity is comparable to the surfatron (at least 2 orders) [24] for sulfur in a thiophene sample and the ICP (at least 2 orders) [16] for Fe in a ferrocene sample.

Minimal Detectable Quantity

The sidearm arrangement was chosen to obtain a MDQ (see Table 8) for ferrocene and dichloro-dimethyl tin without the aid of the DeltaBond phenyl and DeltaBond cyano columns, respectively. The MDQ's were calculated according to

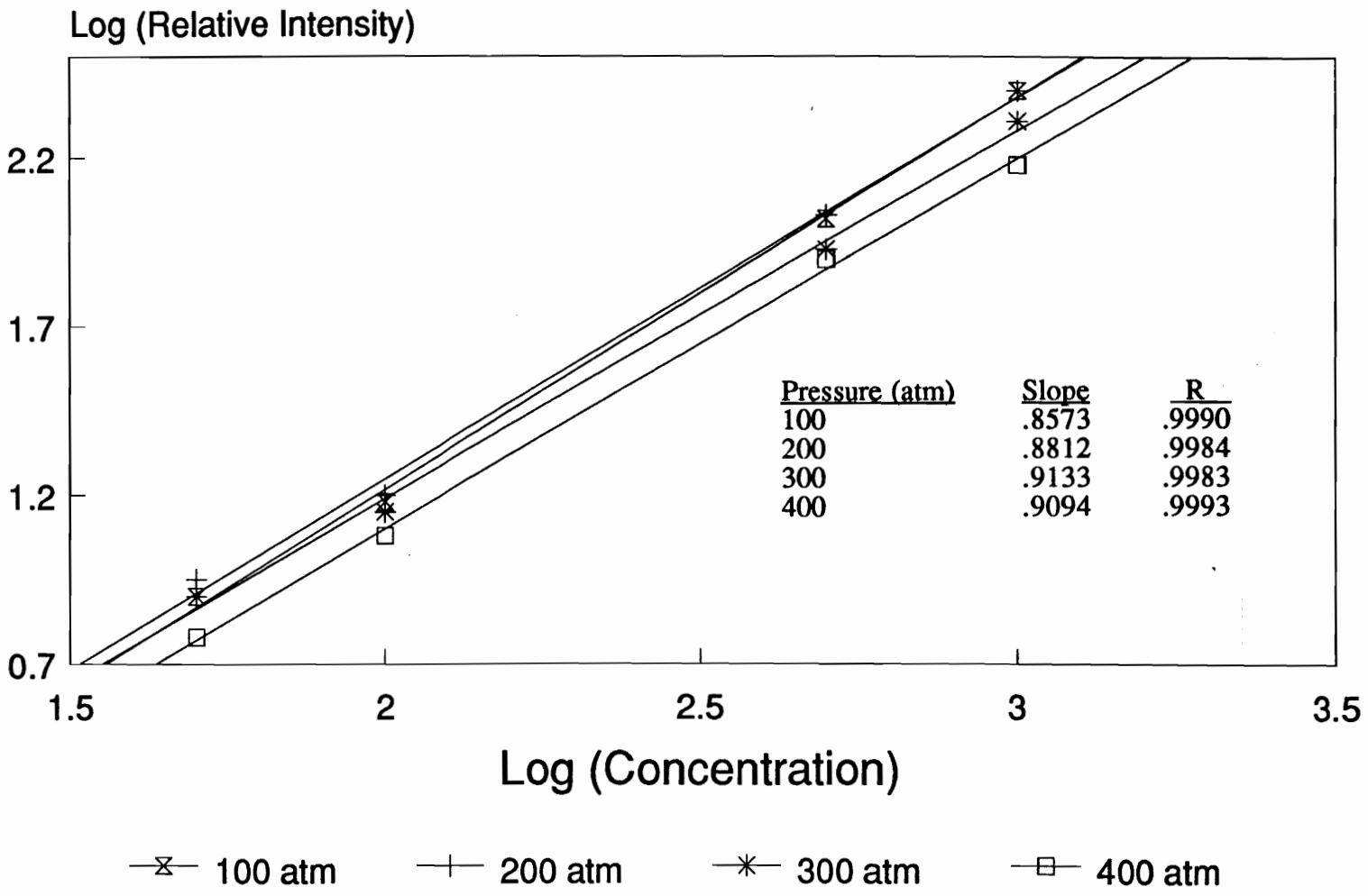

Figure 29: Linear Dynamic Range as a Function of Different Isobaric Pressure

Table 8: MDQ for Sidearm Introduction

	Ar-HEMIP [1]	ICP [2]	ICP [3]
Fe	10 pg (373.8 nm)	60 pg	15 ng/uL (259.9 nm)
Sn	30 pg (270.8 nm)	-	-

[1] This work; C.H. Hartmann, Anal. Chem. 43, 113A (1971).

[2] J.W. Olesik and S.V. Olesik, Anal. Chem. 59, 796 (1987).

[3] C. Fujimoto, H. Yoshida, and K. Jinno, J. Chromatogr. 411, 213 (1987).

reference 35. The experimental conditions were 100 atm, 100% CO_2, 30 um slits (bandpass of 0.96 A), 110^0 C, 373.8 nm line for Fe and 270.78 nm line for Sn, and -800 V on the PMT. Under these conditions the MDQ's were determined to be 10 pg Fe and 30 pg Sn. Jinno et al. [16] have reported a MDQ for iron from a ferrocene sample of 15 ng/uL at 0.5 uL injection and a S/N=4 with the inductively coupled plasma. Also, Olesik and Olesik [15] have reported a limit of detection to be 60 pg for iron from a ferrocene sample with a S/N=3. However, one important point in a comparison of MDQ's is these authors [15, 16] did not give the analytical parameters (number of observations, working curve range and solvent system) under which their MDQ's were estimated.

SUMMARY

The direct introduction of SFC effluent from a packed DeltaBond column has been demonstrated to be feasible with a MIP as an elemental selective detector when the high efficiency TM_{010} cavity was employed. This direct introduction was accomplished by placing the tapered restrictor either through (1) the central tube of the torch or (2) the sidearm of the torch.

When pressure programming experiments are compared for the two sample introduction methods one finds the central

introduction arrangement results in a decreasing background signal with increasing pressure, whereas the sidearm results in an increasing background signal with increasing pressure. The level of background emission is related to the amount of CO_2 being atomized by the plasma, as well as the effect of CO_2 on the tuning of the plasma to the generator. The tuning of the plasma, which determines the energy imparted to the plasma, does not suffer with the sidearm introduction as it does with the central introduction. Using the central introduction and higher Ar flow rates, the background emission decreases, indicating a loss of energy within the plasma. In addition, both could tolerate the addition of organic modifier and never extinguished over all experimental parameters studied. The changing background with increasing pressure or increasing mass flow of CO_2 is attributed to molecular broad band emission, which is the dominate interferent in the UV/VIS region of the spectrum.

Both sample introduction methods gave similar RSD's (3%) for injection-to-injection repeatability. However, restrictor "freezing" and arcing of the plasma are of concern when employing the central tube of the torch but are of no consequence when employing the sidearm configuration.

As the flow rate of SFC mobile phase increased under isobaric conditions, the plasma background emission was

relatively unchanged for both 100% CO_2 and 95% CO_2 with 5% MeOH modifier, but required cavity coupling at each pressure. Therefore, the HEMIP maintained its soundness, with the addition of organic modifier, as an elemental detector.

The Ar-HEMIP demonstrated its ability to detect single component injections. Thus, suggesting supercritical fluid flow injection may be a viable means for nearly 100% sample transport efficiency. However, more importantly it can detect independent components in a mixture which has been separated via SFC.

The two methods of sample introduction were comparable in analytical performance with respect to MDQs. However, the sidearm introduction gave the best performance with a MDQ of 10 pg Fe in a ferrocene sample and 30 pg Sn in an industrial sample of dichloro-dimethyl tin, whereas the central introduction gave 30 pg Fe as its MDQ. Additionally, the sidearm introduction demonstrated a linear dynamic range of at least 3 orders of magnitude.

Chapter 5

THE EVALUATION OF THE He-HEMIP FOR ELEMENT SELECTIVE DETECTION FOR PACKED COLUMN SFC

In this chapter, the coupling of the He-HEMIP and an Ar-HEMIP to a packed column SFC will be described. The effect of the introduction of supercritical CO_2 on the plasma excitation temperature, electron number density, plasma geometry, and cavity coupling will be reported. For nonmetal species, the selection of emission lines used will be noted. Studies of the effect of plasma gas flow rates, plasma position, and applied power will be discussed. MDQ values for S, P, and Cl will be presented. Also the effect of plasma gas flow rates and pressure programming on these values will be presented.

Experimental

Reagents

The following information is to supplement the information in Chapter 2. Thiophene was purchased from Aldrich as 99+ % and used without further purification. Paraoxon was purchased from Chemical Service, Inc., West Chester PA.

Viewing Geometry

Traditionally, the most sensitive spectral emission from an Ar-MIPs is found using radial (side-on) (Figure 9) viewing of the plasma. This mode is employed because the predominate analyte emission occurs outside the cavity in the plasma tail when using argon as the plasma gas. Radial viewing also offers improved selectivity [37], because both vertical and lateral profiles of the plasma tail are possible allowing spatial resolution of various analyte species (ie non-refractory vs. refractory).

However, when helium is employed as the plasma gas the axial mode (end-on) (Figure 9) is preferred. It should be noted that the helium discharge is considerably smaller than that of the Ar discharge in the HEMIP cavity and a luminous plasma tail is not observed to extend outside of the cavity. Also, this mode offers improved analytical sensitivity [37] which is necessary for the detection of nonmetals and halogens. Further, the axial mode for helium is used because the plasma is optically transparent in the radial mode. But, this mode affords improved sensitivity since the cross-section of the plasma discharge monitored offers a greater density of excited state analyte. Therefore, the axial mode will be employed for this chapter.

Excitation Temperature

The excitation temperature of the helium plasma as a function of CO_2 flow rate was measured by the slope method [50]. This method involves the monitoring of emission intensities of 10 Fe lines, each line representing the relative population of an Fe excited state. The iron was introduced into the plasma as an aqueous species using a Meinhard nebulizer and Scott spray chamber. A desolvation system was not employed in the introduction of aqueous sample for the HEMIP cavity. The error associated with the temperature measurements is 3%.

Electron Number Density

The electron number density of the helium plasma as a function of CO_2 flow rate was measured by the width of the hydrogen-beta line (486.13 nm) at half height and calculated according to Griem [42]. It is important to point out that the values obtained from these measurements should not be directly compared to other n_e for MIP systems because only a medium resolution monochromator was employed in these studies. These values are useful in assessing the effect of CO_2 on the plasma.

Results and Discussion

Effects of CO_2 on Excitation Temperature

Although the exact effects of carbon species on atomic spectrometric signals have not been entirely determined among atomic spectroscopists, it has been noted that the combustion and decomposition products of carbon containing species (acetylene, propane, and CO_2) absorb plasma energy [28, 44, 45] and thus result in diminished atomic emission signals of the analyte in argon plasmas. This effect of organic species on the plasma temperature of the helium HEMIP is described in Table 9. In this table the plasma excitation temperature, determined using the slope method with aqueous Fe [50] is shown with the introduction of 0 mL/min, 70 mL/min and 120 mL/min of CO_2 into the plasma gas. These flow rates represent CO_2 flows of 0%, 7% and 12%, respectively. With the introduction of CO_2, the plasma temperature is noted to drop by 250 K. Since the error in these measurents is 3%, this difference is not statistically different (3 sigma). Unlike the Ar plasma in which the excitation temperature dropped 30% with the introduction of CO_2 [4], the He plasma appears to be relatively unaffected by the gas, and for this reason, may function as a more precise elemental plasma detector than an Ar based system.

Table 9: Effect of Carbon Dioxide on Exictation Temperature

Helium Flow Rate (1 L/min)	T(exc), (K)
He + Carbon Dioxide (0 mL/min)	6300
He + Carbon Dioxide (70 mL/min)	6100
He + Carbon Dioxide (120 ml/min)	6100

Effects of CO_2 on Electron Number Density

Although the exact excitation mechanism for atomic emission spectroscopy in microwave induced plasmas is not unanimously agreed upon, the electron number density is helpful in making predictions of the performance of the plasma under different analytical conditions. In this study, the measured electron number density for a He plasma is calculated to be 5 X 10^{14} e^-/cc (Table 10). It should be noted that this value does not change with the addition of CO_2, whereas the number density fell by a factor of 10 for an Ar-HEMIP under similar conditions [28]. These data suggest that the helium plasma contains enough energy to maintain its robustness even when organic gases are added.

The Effect of CO_2 on Plasma Geometry

Although the plasma discharge of the Ar-HEMIP did not show evidence of constriction with the addition of CO_2 [29], the plasma discharge of the He-HEMIP does constrict in size upon the addition of CO_2 to the plasma. When operated with He only or with the addition of nebulized aqueous samples, the plasma discharge fills the plasma torch. This diameter is approximately 5 mm. When the CO_2 is introduced into the plasma, the constriction occurs. Figure 30, a lateral profile of the plasma (monitored with time) is shown, where plot A is the observed plasma emission background (set at

Table 10: Effect of Carbon Dioxide on Electron Number Density

Helium Flow Rate (1 L/min)	N_{e^-} (e^-/cc)
He + Carbon Dioxide (0 mL/min)	5.3 E+14
He + Carbon Dioxide (70 mL/min)	5.3 E+14
He + Carbon Dioxide (120 ml/min)	--

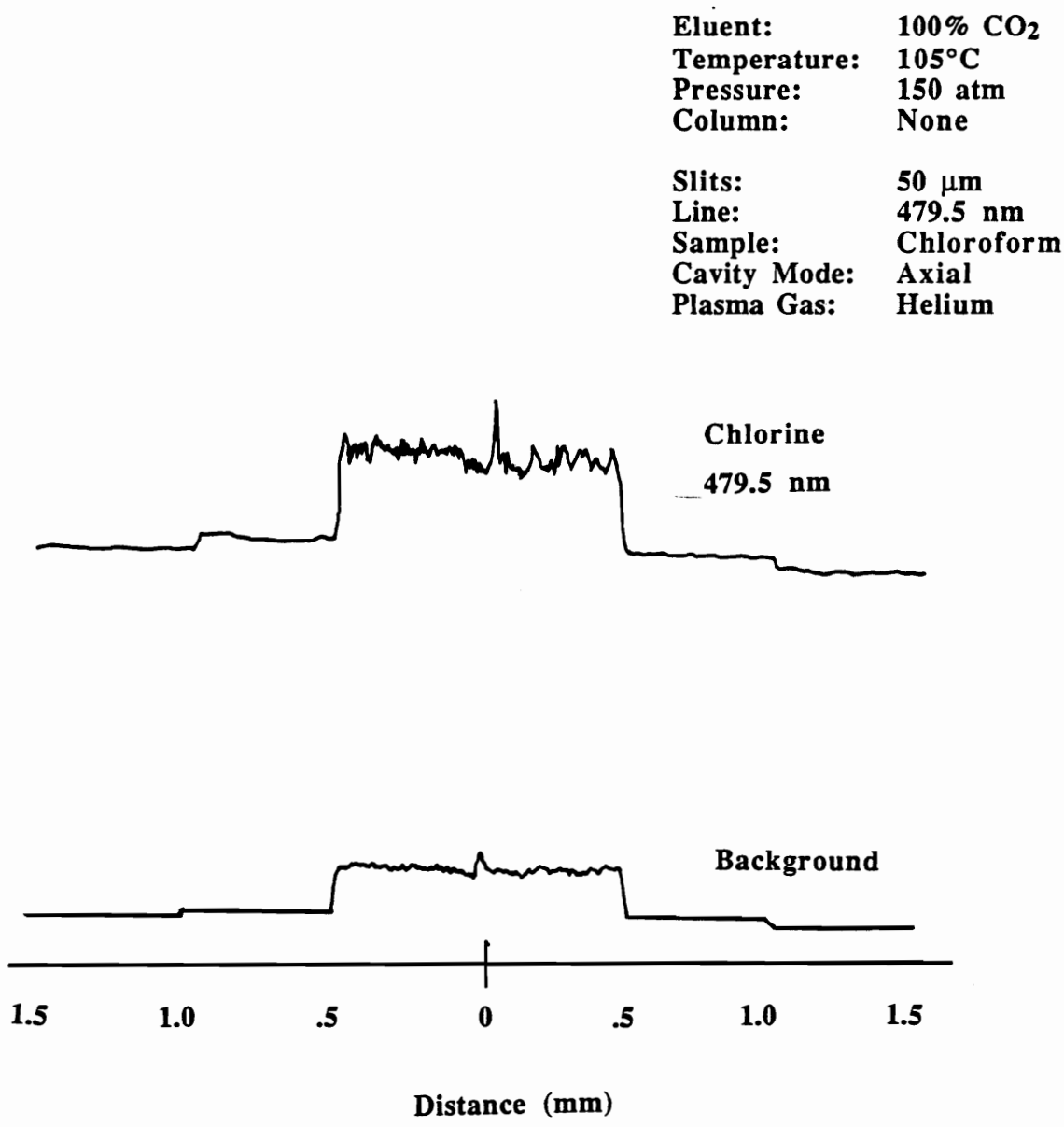

Figure 30: Lateral Profile of the Axial Plasma

the Cl emission line of 479.5 nm) with the addition of CO_2 to the plasma gas, and plot B is the observed chlorine emission with the addition of CO_2. These plots illustrate that the plasma is no longer 5 mm wide, but is constricted to approximately 1mm in width with the addition of CO_2. Therefore, there is approximately 2.5 mm annular distance, dictated by the torch dimensions, about the plasma where the analyte can skirt the plasma discharge. This skirting may result in a loss of analytical sensitivity.

Cavity Coupling

The coupling of the cavity to the generator plays an important role in power transfer efficiency [8] and ultimately in the analytical performance of the MIP. Figure 31 demonstrates the effect of the cavity not being critically coupled over all pressures of a SFC pressure ramp. These observations are made using a phosphorus emission line. To the left of the plot the background emission level starts to increase at 150 atm and continues to increase until approximately 270 atm, where due to the increased mass of CO_2 being introduced into the plasma, the cavity is no longer critically coupled. At this point (270 atm) the background emission level greatly decreases due to a power loss to the cavity and continues until the pressure ramp terminates at 350 atm.

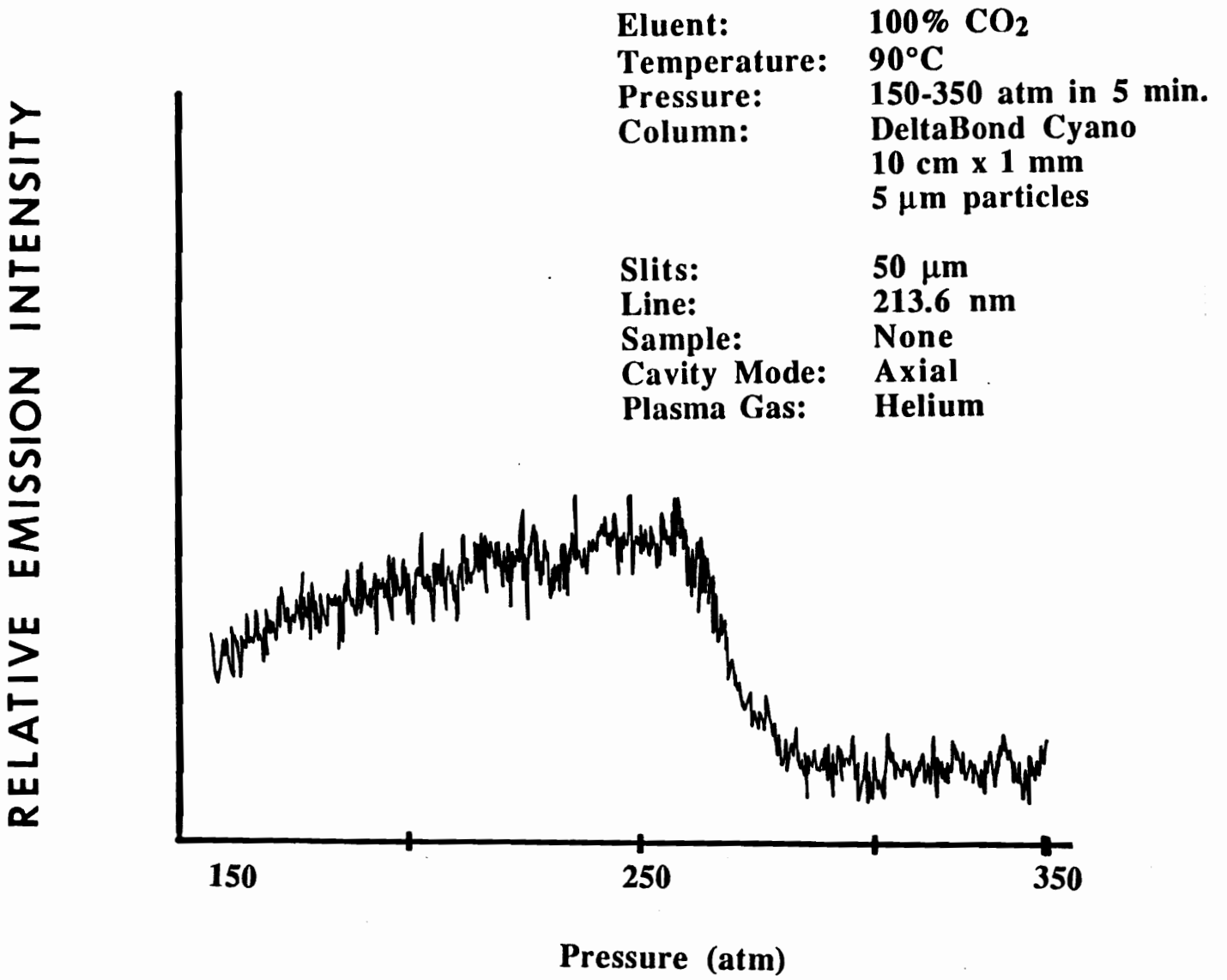

Figure 31: Effect of Pressure Programming on Background Emission on an Improperly Tuned Cavity (1 inch= 0.1 V)

In Figure 32, the pressure ramp is run again, with the cavity being adjusted to achieve critical coupling at 350 atm. Under these conditions the background emission level continued to increase as the pressure ramp increased. This effect is the result of an increase in molecular background emission as the mass flow of CO_2 increases with pressure.

Line Selectivity

A chlorine headspace generator, Figure 33, was used to provide a constant source of analyte to the plasma for line selection. Figure 34 shows a scan from 477 nm to 486 nm which contains three chlorine lines. These lines are 479.5 nm (A), 481.0 nm (B), and 481.9 nm (C). These data illustrate that the line at 479.5 nm is the most intense line, thus it was selected for all chlorine measurements. A similar procedure was followed for determining the visible emission lines for P and S.

Effects of Plasma Flow Rate on S/N

The flow rate of the plasma gas plays an important role in the performance of the He-HEMIP with respect to S/N. Figure 35 demonstrates that as the plasma gas flow rate is decreased from 2.2 L/min to 0.8 L/min, the S/N ratio continually improves. Therefore, the lower flow rates seem desirable, but this lower plasma gas flow diminishes the

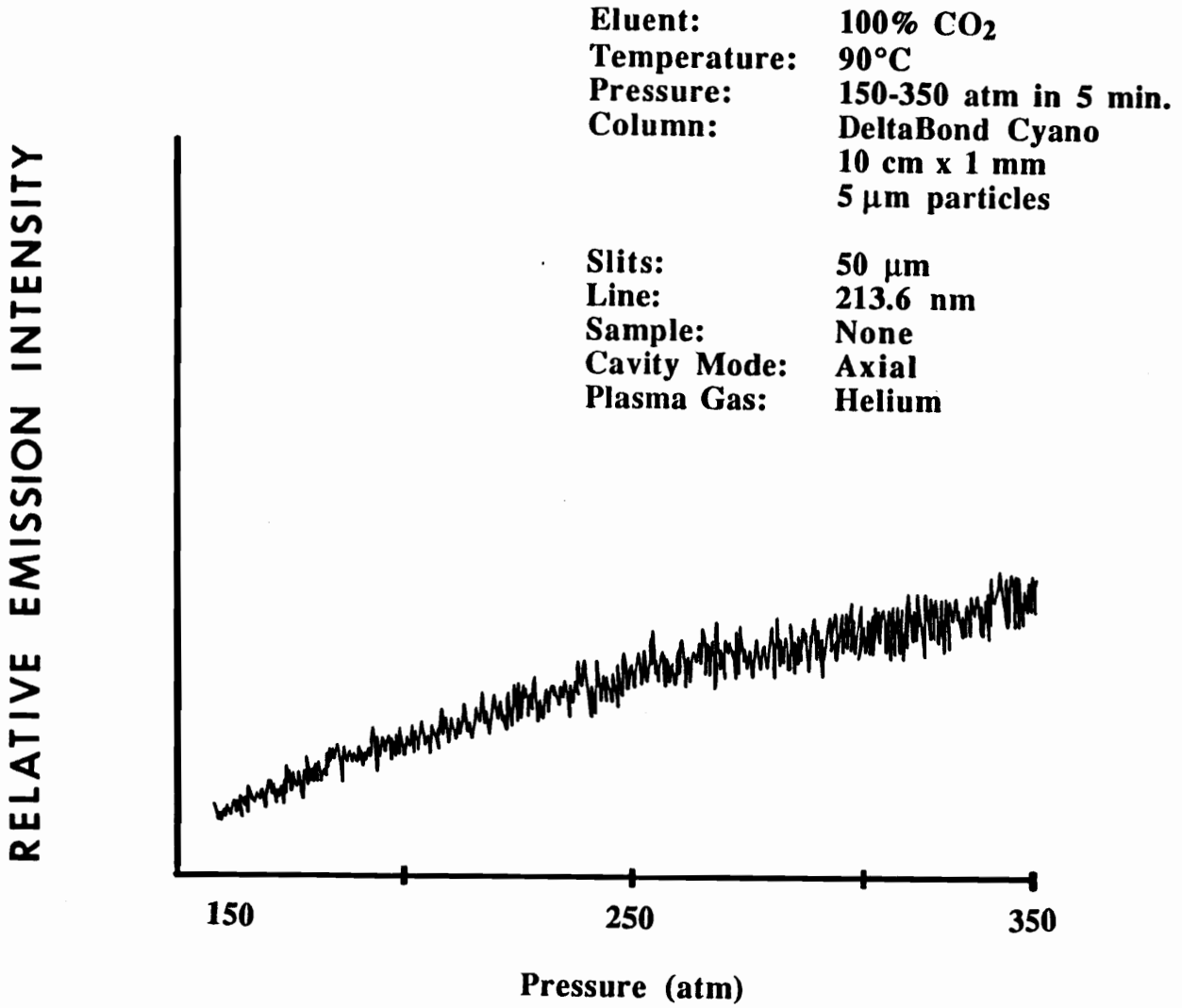

Figure 32: Effect of Pressure Programming on Background Emission on a Properly Tuned Cavity (1 inch= 0.1 V)

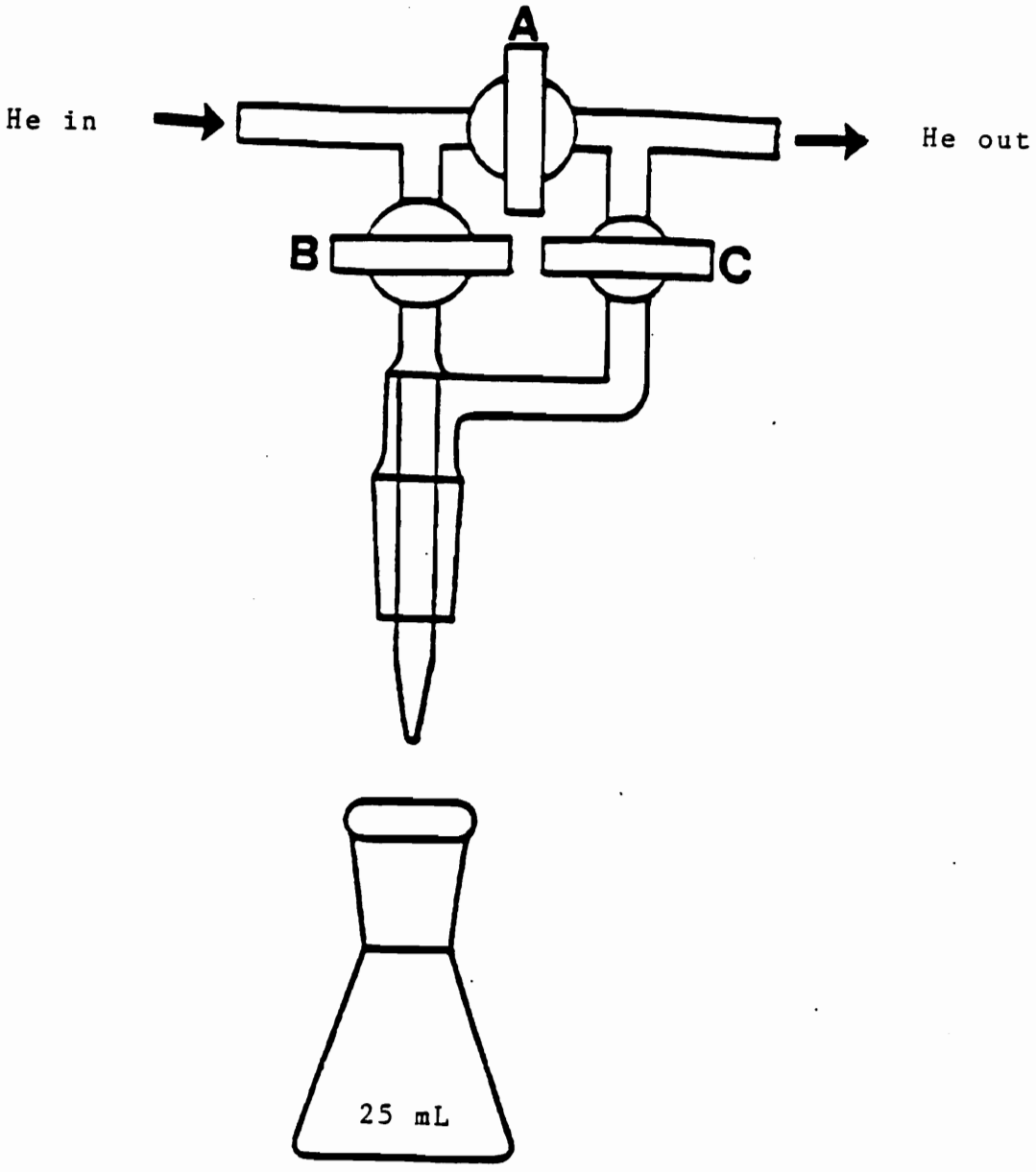

Figure 33: Schematic of Head Space Generator

Scan: 477 to 486 nm
Sample: Chloroform headspace for chlorine source
Slits: 30 μm
Cavity Mode: Axial
Plasma Gas: Helium

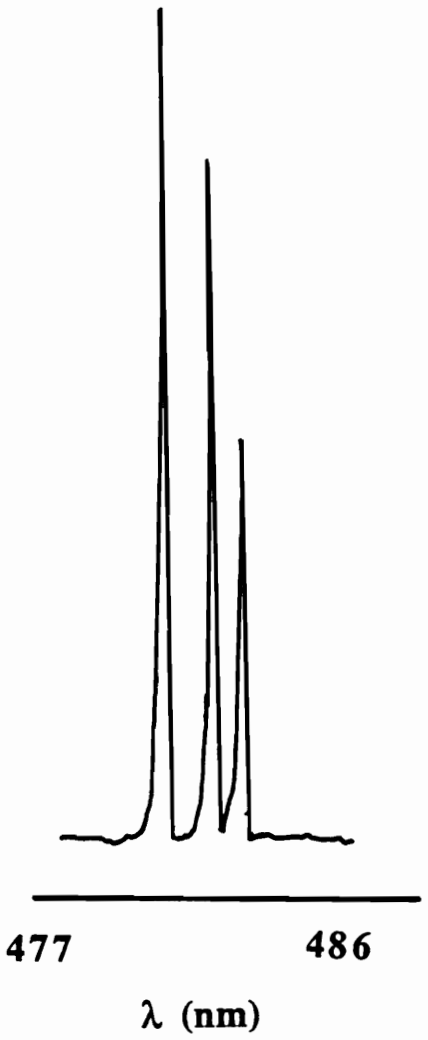

Figure 34: Scan of Cl Lines

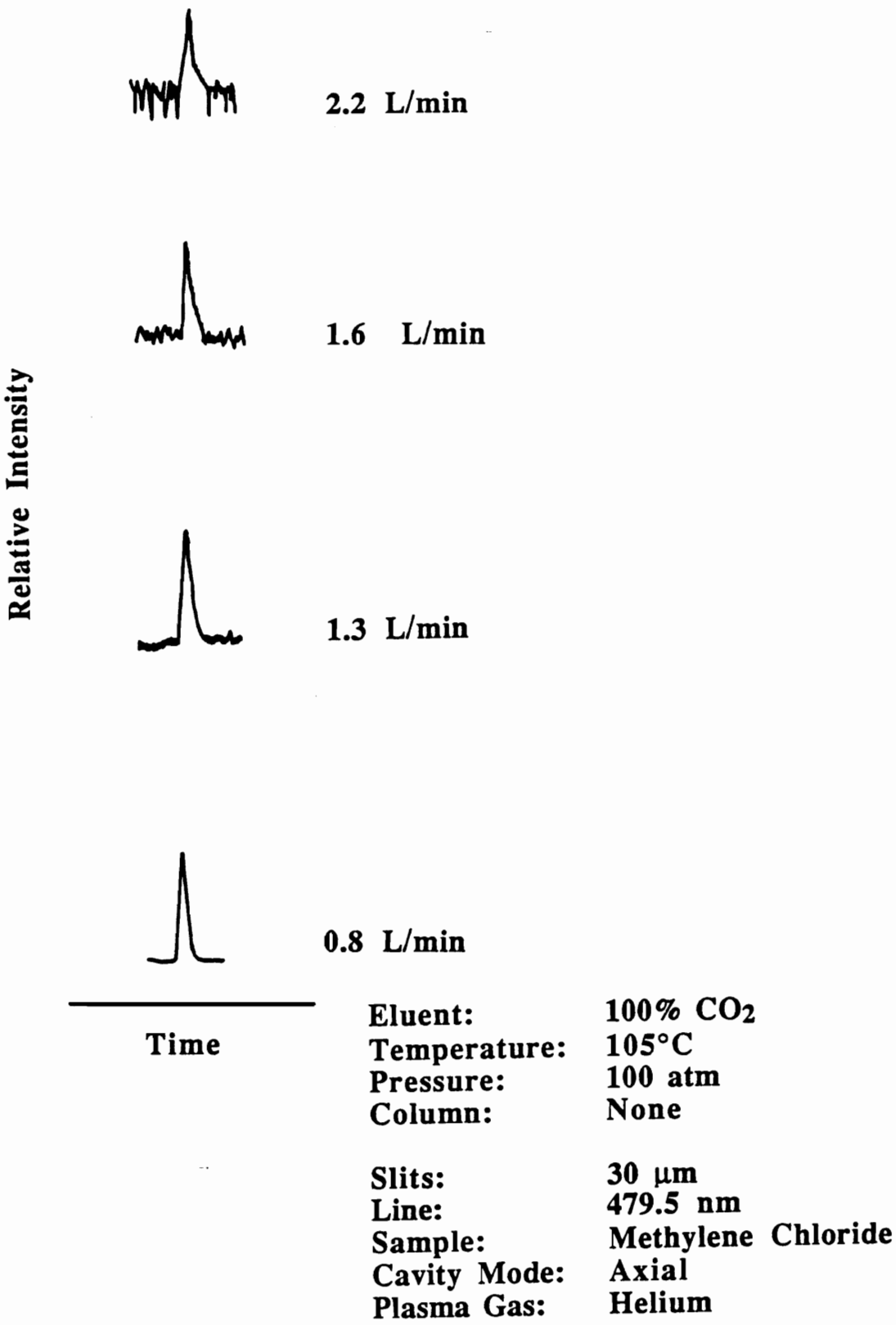

Figure 35: Effect of Plasma Flow Rate on S/N Ratio for Cl Emission

cooling of the torch which can lead to the melting of the plasma torch. Therefore, consideration is being given to the redesigning of the torch to accommodate the lower flows without detrimental effects to the lifetime of the torch.

Effect of Plasma Position on S/N

The axial profile of the helium plasma in Figure 36 shows the effect of the plasma position on the S/N ratio of a sulfur containing analyte where each peak represents an independent injection. These data suggest that the optimum positioning of the plasma with respect to the monochromator entrance slit is approximately the center (0 mm) of the plasma discharge.

If significant skirting of the excited species about the plasma discharge was occurring, then the optimum signal should have been located off-center. However near the 0 position the signal appears to be maximized, while the noise is unchanged. Therefore, this suggests a new torch design (see Appendix) could reduce the plasma flow rate and increase the analyte residence time. This would reduce the probability of the analyte missing the plasma, thus increasing the analytical sensitivity.

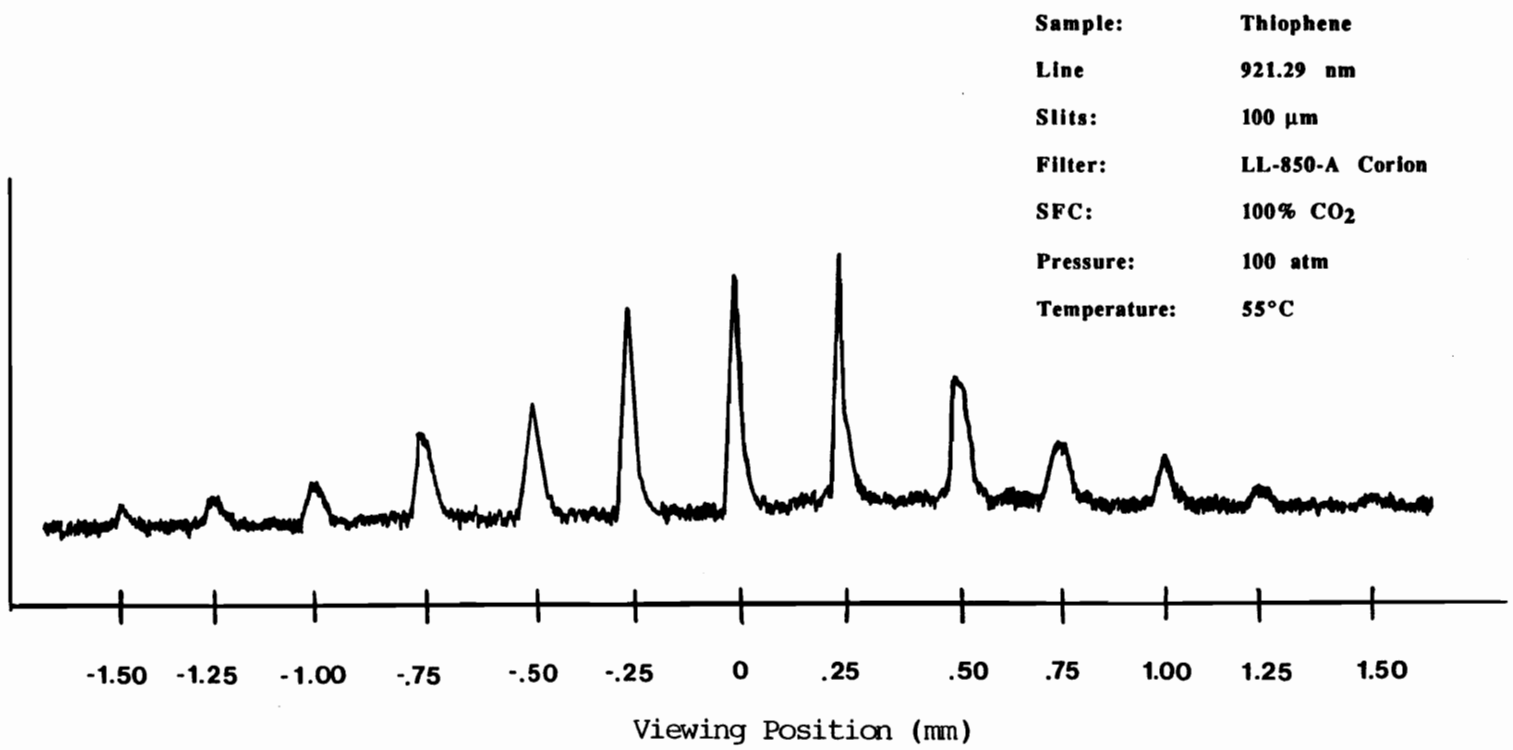

Figure 36: Effect of Plasma Viewing Position on Analyte Signal

Effect of Applied Power on S/N

The effect of applied power on S/N ratios for a S containing (thiophene) analyte is shown in Figure 37. It can be seen in this figure that a loss of S/N occurs when the power exceeds 150 W. Below the 150 W level, the helium HEMIP is prone to being extinguished. Therefore, 150 W was chosen as the optimum applied power for all studies using the He-HEMIP.

Effects of Plasma Flow and Chromatographic Pressure on MDQ

A 3-D plot of MDQ, chromatographic pressure and plasma flow for a chlorine containing analyte is presented in Figure 38. As can be determined from this figure, there is no statistical difference (factor of 3) in the MDQs with respect to pressure for the 2 L/min and the 3 L/min He plasma flow rates. These MDQ levels are in accordance with Hartmann's procedures for GC measurements [35]. However, this trend is not true for the 1 L/min He plasma flow, which exhibits a statistical change in the MDQ as a function of chromatographic pressure. This change is accounted for by the plasma size at 1 L/min which is approximately 3 mm wide, thus allowing approximately 1.5 mm annular distance for the analyte to miss the plasma. Also, the plasma is not as visibly intense when compared to the other two flow rates.

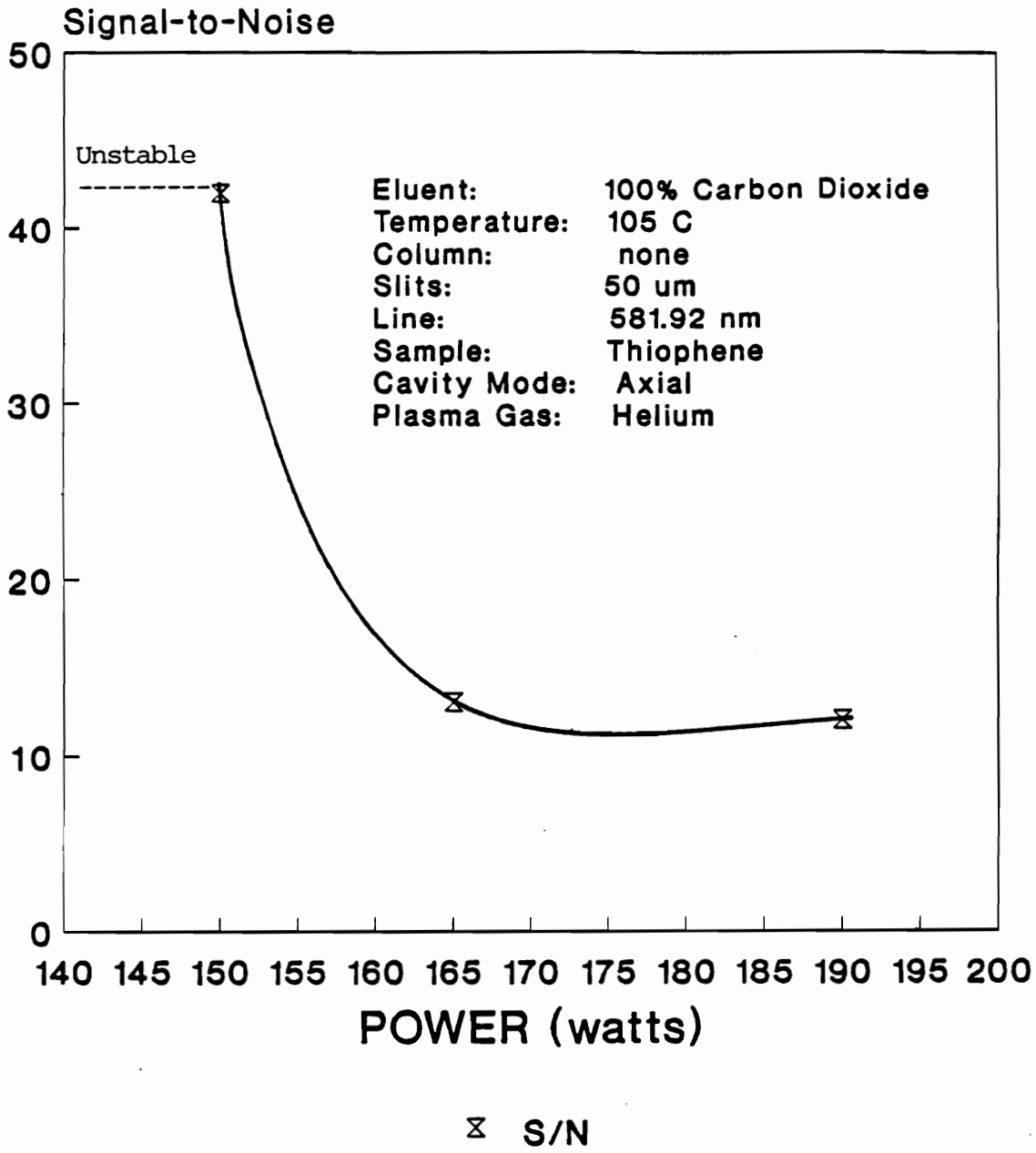

Figure 37: Effect of Applied Power on S/N Ratio

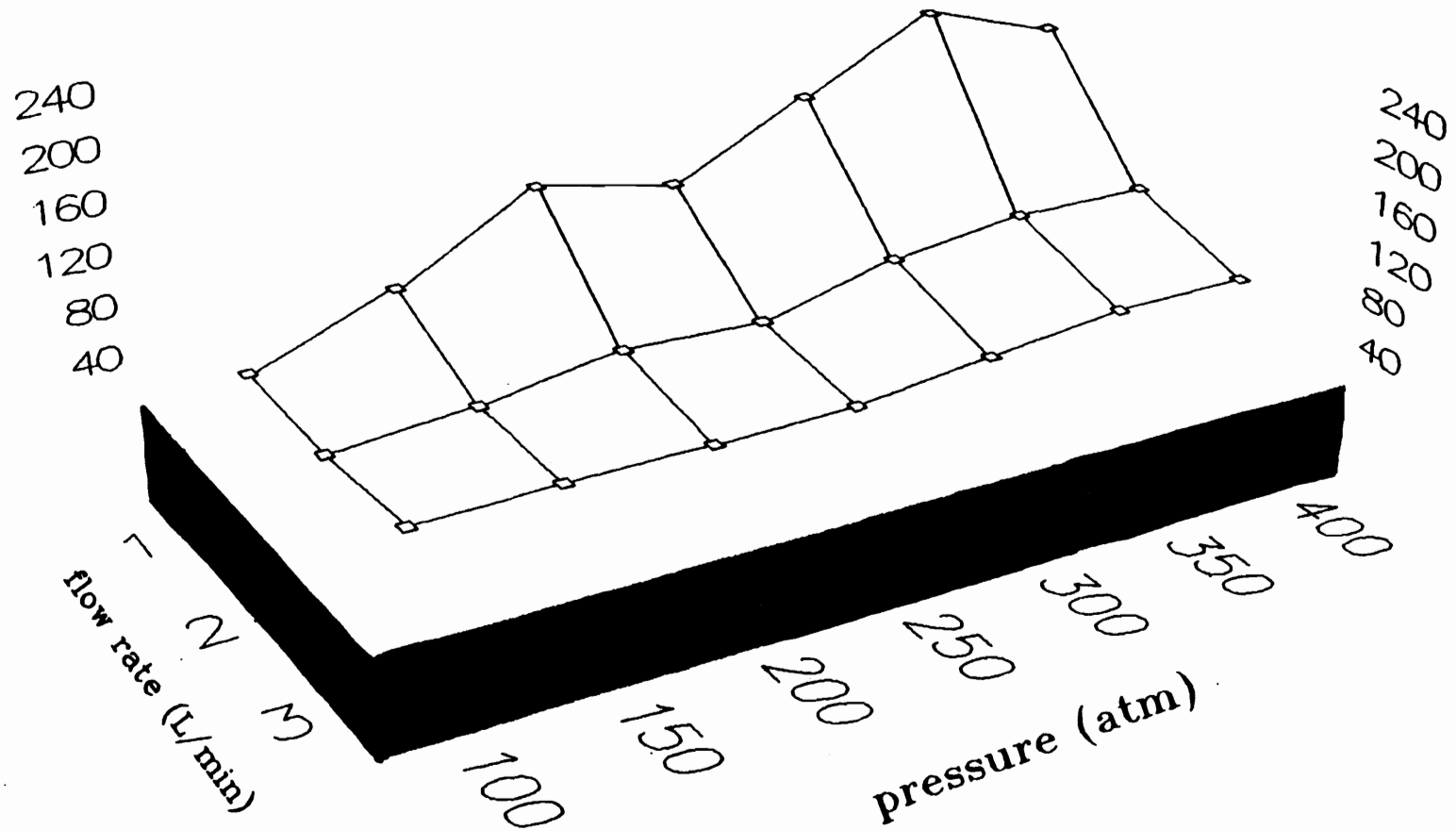

Figure 38: Effect of Plasma Flow Rate and Chromatographic Pressure on MDQ for Sulfur

Effects of Plasma flow and Chromatographic Pressure on S/N

This measurement of S/N takes into consideration the noise of the entire experimental system, not just the noise of the detector as with the MDQ data previously mentioned. The effect of plasma flow and chromatographic pressure on the S/N ratio of a chlorine sample is shown in Figure 39. This plot illustrates that there is no difference (factor of 3) in the S/N as a function of pressure or plasma flow, except at 100 atm and 1 L/min. Under these conditions the S/N is a maximum but decreases as the pressure increases. Since the mass flow of CO_2 increases with increasing pressure, the noise of the system grows while the signal remains relatively constant, thus giving a net loss in the S/N ratio with increasing pressure.

Reported MDQs

Table 11 gives the MDQ for S (thiophene), Cl (methylene chlorine) and P (Paraoxon). These MDQs were calculated using the method set forth in reference 35. The experimental parameters employed for these measurements were as follow: 100 atm isobaric pressure, -800 V PMT, 50 um slits, current-to-voltage convertor at 10^{-6} A/V sensitivity and 105 ^{o}C. Under these experimental conditions the MDQs were 50 ng for Cl, 30 ng for S and 0.1_3 ng for P while monitoring lines 479.5 nm, 581.9 nm and 255.3 nm

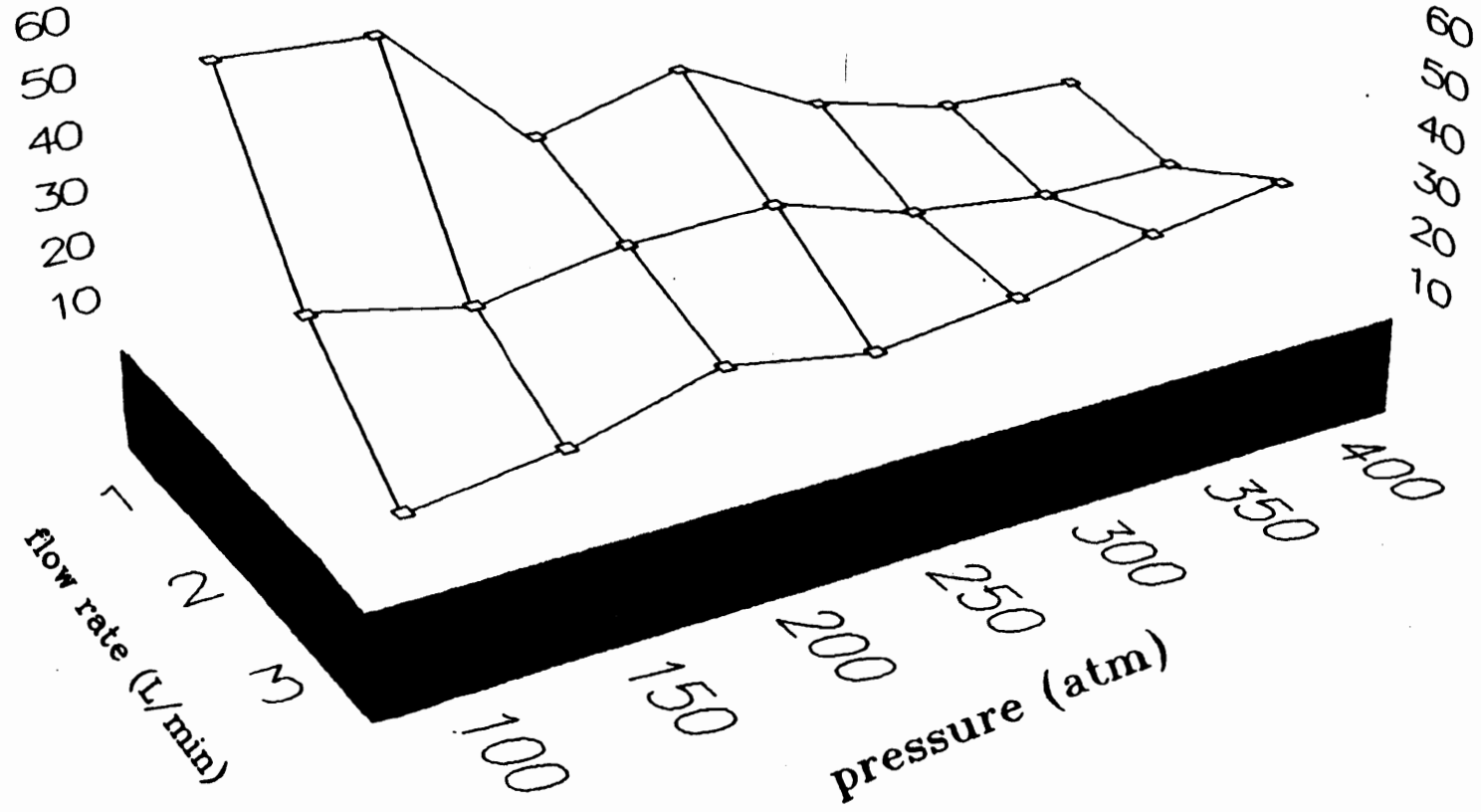

Figure 39: Effect of Plasma Flow Rate and Chromatographic Pressure on S/N for Sulfur

Table 11: MDQ for Chlorine, Sulfur, and Phosphorus with the He-HEMIP

Element	Wavelength (nm)	MDQ (ng)
Cl	479.5	50
P	255.3	0.1
S	180.7	50
	581.9	30
	921.2	30

respectively. In addition, the MDQ for S was determined to be 50 ng and 30 ng at 180.7 nm (Ar purged) and 921.2 nm respectively.

SUMMARY

In this chapter, a He-HEMIP has been evaluated as an element selective detector for SFC. The excitation temperature and electron number density are shown not to be affected by the introduction of CO_2 as Ar plasmas are. Optimum applied power to the cavity is found to be 150 W. Although the plasma constricts in diameter with the addition of CO_2, the maximum analyte emission is found to occur in the center of the plasma discharge. MDQ levels for nonmetals are determined and found to be in low to sub ng level. The use of pressure programming is shown not to affect the MDQ at higher plasma gas flow rates. At low flow rates, an increase in MDQ levels is noted with the increase in the SFC pressure ramp. In a similar fashion, S/N ratios are only affected at low plasma gas flow rates when pressure ramps for the CO_2 gas are used.

CHAPTER 6

CONCLUSIONS

The major objective of the work described in this dissertation was to address the need of a "multi-element" detector for supercritical fluid chromatography. The HEMIP was evaluated as an element selective detector for packed column SFC. The HEMIP cavity has been demonstrated to provides a significant low power advantage when compared to other microwave induced plasmas. It also can be critically coupled thus minimizing reflected power. Therefore, this system can tolerate the polar organic modifiers that are often used in packed column SFC.

The Ar-HEMIP is affected by the introduction of CO_2. This perturbation of the plasma was monitored through the determination of the electron number density and the plasma excitation temperature. The electron number density of the plasma initially decreased with the introduction of CO_2 and then leveled off. However, the excitation temperature of the plasma continually decreased with the addition of CO_2. The decrease in these two parameters indicated that the Ar plasma possessed a lesser excitation energy with the addition of CO_2 and hence reduced atomic emission signals.

The sample introduction of SFC effluent into the plasma was accomplished by two means. The method of central introduction, although the simplest to perform, required caution due to the arcing of the plasma to the restrictor, and the possibility of the restrictor freezing from the expansion of the CO_2 gas. Alternatively, the method of sidearm introduction eliminated these problems and led to superior analytical performance. Both configurations could maintain isobaric pressure separations and separations using pressure programming with 100% CO_2 or polar organic modified CO_2. In addition, both sample introduction techniques resulted in a 3% RSD for manual injections. Finally, the sidearm configuration permitted elemental sensitivities in the picogram range, which is compatible to the use of the inductively coupled plasma. The Ar-HEMIP demonstrated a linear dynamic range of at least three orders of magnitude. Also, it was shown the UV/VIS region was prone to molecular broad band emission interference, thus requiring great care in line selection or a movement of observed wavelength to the near IR. This region of the spectrum has been reported to be less prone to molecular broad band emission interference, since a short wavelength filler can be used to block out emission below 900 nm.

Another area of great interest is the ability to detect not only metals but nonmetals. The He-HEMIP shows great

promise as an element selective detector for metal and nonmetal containing effluent from packed column SFC. The MDQ for metals was improved by a factor of 10, when compared to the Ar-HEMIP. Also, the MDQ for Fe, Sn, S, P, and Cl were in the subnanogram to picogram range.

The He plasma, unlike Ar, constricts with the addition of CO_2, which resulted in a slight loss of sensitivity at higher pressure and lower plasma flow rates. Also, as the plasma flow rate decreased, the S/N ratio increased, with the noise showing the greatest change; that is, the magnitude of the noise was a function of the tangential flow of the plasma gas and it decreased and the plasma gas flow decreased. These two facts have led to the need for a new torch design. This design should minimize these limitations. The plasma viewing position was also shown to affect the S/N ratio with the maximum being near the center of the plasma discharge.

To overcome analytical limitations, it is thought among some researchers in this field that increasing the applied power leads to better sensitivity. However, in this study the opposite was found to be the case. That is, the S/N ratio decreased after the optimum power level was surpassed, regardless of cavity coupling. Finally, it was shown that

cavity coupling plays a major role in the atomic emission spectroscopy performance of the HEMIP.

The work presented in this dissertation provides an overview of the HEMIP's ability to address element speciation in SFC. The high sensitivity and the ability to tolerate polar organic modifiers make the He-HEMIP a potentially powerful analytical detector for chromatography.

REFERENCES

1. C. I. M. Beenakker, Spectrochim. Acta **31B,** 483 (1976).

2. C. I. M. Beenakker, Spectrochim. Acta **32B,** 173 (1977).

3. P. C. Uden, Chromatogr. Forum **1,** 17(1986).

4. T. H. Risby and Y. Talmi, CRC Crit. Rev. Anal. Chem. **14,** 231(1983).

5. L. Ebdon, S. Hill and R. W. Ward, Analyst(London) **111,** 1113(1986).

6. A. H. Mohamad and J. A. Caruso, Adv. Chromatogr. **26,** chaper 5(1987).

7. P. N. Keliher, D. J. Gerth, J. L. Synder, H. Wang and S. F. Zhu, Anal. Chem. **56,** 786R (1988).

8. L. G. Matus, C. B. Boss and A. N. Riddle, Rev. Sci. Instrum. **54,** 1667 (1983).

9. D. L. Haas and J. A. Caruso, Anal. Chem. **56,** 2014 (1984).

10. D. L. Haas, J. W. Carnahan and J. A. Caruso, Appl. Spectrosc. **37,** 82 (1983).

11. K. B. Kull and J. W. Carnahan, Appl. Spectrosc. **42,** 1061 (1988).

12. G. L. Long and L. D. Perkins, Appl. Spectrosc. **41,** 980 (1987).

13. L. D. Perkins and G. L. Long, Appl. Spectrosc. **42,** 1285 (1988).

14. L. D. Perkins and G. L. Long, Appl. Spectrosc. **43,** 499 (1989).

15. R. F. Browner and A. W. Boorn, Anal. Chem. **56,** 786A (1984).

16. R. F. Browner and A. W. Boorn, Anal. Chem. **56,** 875A (1984).

17. J. M. Levy and W. M. Ritchey, J. Chrom. Sci. **24,** 242(1986).

18. T. H. Gouw and R. E. Jentoff, J. Chromatogr. **68,** 303(1972).

19. J. C. Giddings, M. N. Meyers, L. McLaren and R. A. Keller, Science **162,** 67(1968).

20. J. C. Fjeldsted, R. C. Kong and M. L. Lee, J. Chromatogr. **279,** 449(1983).

21. T. L. Chester, J. Chromatogr. **299,** 424(1984).

22. B. E. Richter, HRC & CC **8,** 297(1985).

23. T. Greibrokk, B.E. Berg, A.L. Blilie, J. Doehl, A. Farbrot and E. Lundanes, Anal. Chimica Acta **196,**429 (1987).

24. M. Ashraf-Khorassani, J. W. Hellgeth and L. T. Taylor, Anal. Chem. **59,** 2077(1987).

25. J. W. Olesik and S. V. Olesik, Anal. Chem. **59,** 796 (1987).

26. C. Fujimoto, H. Yoshida and K. Jinno, J. Chromatogr. **411,** 213 (1987).

27. D. Luffer, L. Galante, L. David, M. Novonty and G. Hieftje, Anal. Chem. **60,** 1365 (1988).

28. C. B. Motley, M. Ashraf-Khorassani and G. L. Long, Appl. Spectrosc. **43,** 737 (1989).

29. C. B. Motley and G. L. Long, Appl. Spectrosc. in press.

30. B. W. Smith and M. L. Parsons, J. Chem. Educ, **50,** 679 (1973).

31. H. E. Schwartz, P. J. Barthel and S. E. Morring, HRC&CC **10,** 668 (1987).

32. A. C. Rosselli, D. S. Boyer and R. K. Houck, J. Chromatogr. **465,** 11 (1989).

33. T. L. Chester, D. P. Innis and G. D. Owens, Anal. Chem. **57,** 2243 (1985).

34. R. D. Deutsch and G. M. Hieftje, Appl. Spectrosc. **39,** 214 (1985).

35. C. H. Hartmann, Anal. Chem. **43,** 113A (1971).

36. G. L. Long and J. D. Winefordner, Anal. Chem. **55,** 713A (1983).

37. S. R. Goode and L. K. Kimbrough, Appl. Spectrosc. **42,** 1011 (1988).

38. I. Reif, V. A. Fassel and R. N. Kniseley, Spectro. Acta, **28B,** 105 (1972).

39. B. W. Smith and M. L. Parsons, J. Chem. Ed., **50,** 679 (1973).

40. B. M. Joshi and R. D. Sacks, Anal. Chem., **51,** 1781 (1979).

41. H. R. Griem, Plasma Spectroscopy (McGraw-Hill, New York, 1964).

42. H. R. Griem, Spectral Line Broadening by Plasmas (Academic Press, New York, 1974).

43. C. R. Vidal, J. Cooper, and E. W. Smith, Astrophys. J. Suppl. Series **215,** 37-136 (1973).

44. M. W. Blades and B. L. Caughlin, Spectrochim. Acta, **40B,** 579 (1985).

45. J. S. Bolton, Ph.D. Dissertation, VPI & SU, September 1988.

46. J. S. Bolton and G. L. Long, Spectrochim. Acta, **42B,** 581 (1987).

47. M. Ashraf-Khorassani and L. T. Taylor, Anal. Chem. **60,** 1529 91988).

48. G. L. Long and J. D. Winefordner, Anal. Chem. **55,** 712A, (1983).

49. C. Fujimoto, H. Yoshida and K. Jinno, J. Microcolumn Separation **Jan/Feb,** 19 (1988).

50. D. J. Kalnicky, V. A. Fassel, and R. N. Kniseley, Appl. Spectrosc. **31,** 137 (1977).

APPENDIX

NEW "COOLED TORCH" DESIGN FOR He-HEMIP-SFC

The new torch design (Figure A) is based on reducing the inner diameter of the torch and the plasma flow rate. Due to the heat of the He plasma at low flow rates the quartz torch must be cooled.

Figure A shows the new torch design. The inner quartz tube is 1.5 mm i.d., 2.0 mm o.d., and 9 cm long with a cooling quartz sleeve tube (3.0 mm i.d., 8 mm o.d. and 9 cm long). The distance between the inner diameter of the outer tube and the outer diameter of the inner tube allows a coolant to pass through, thus dissipating the heat from the plasma wall.

Several coolants have been investigated. The first coolant tried was water but this choice prevented the ignition of the plasma due to the absorbance of microwave energy by the OH bonds of water. Next, 50% water 50% ethylene glycol was tried and the plasma could be ignited but required higher powers. Finally, "Wesson Oil" was employed with success. It was necessary to heat the oil to 100 ^{o}C so the circlator could pump the coolant. The "cooled torch" housing the He plasma remained ignited, while the SFC was pressure ramped from 100-400 atmospheres. Elemental

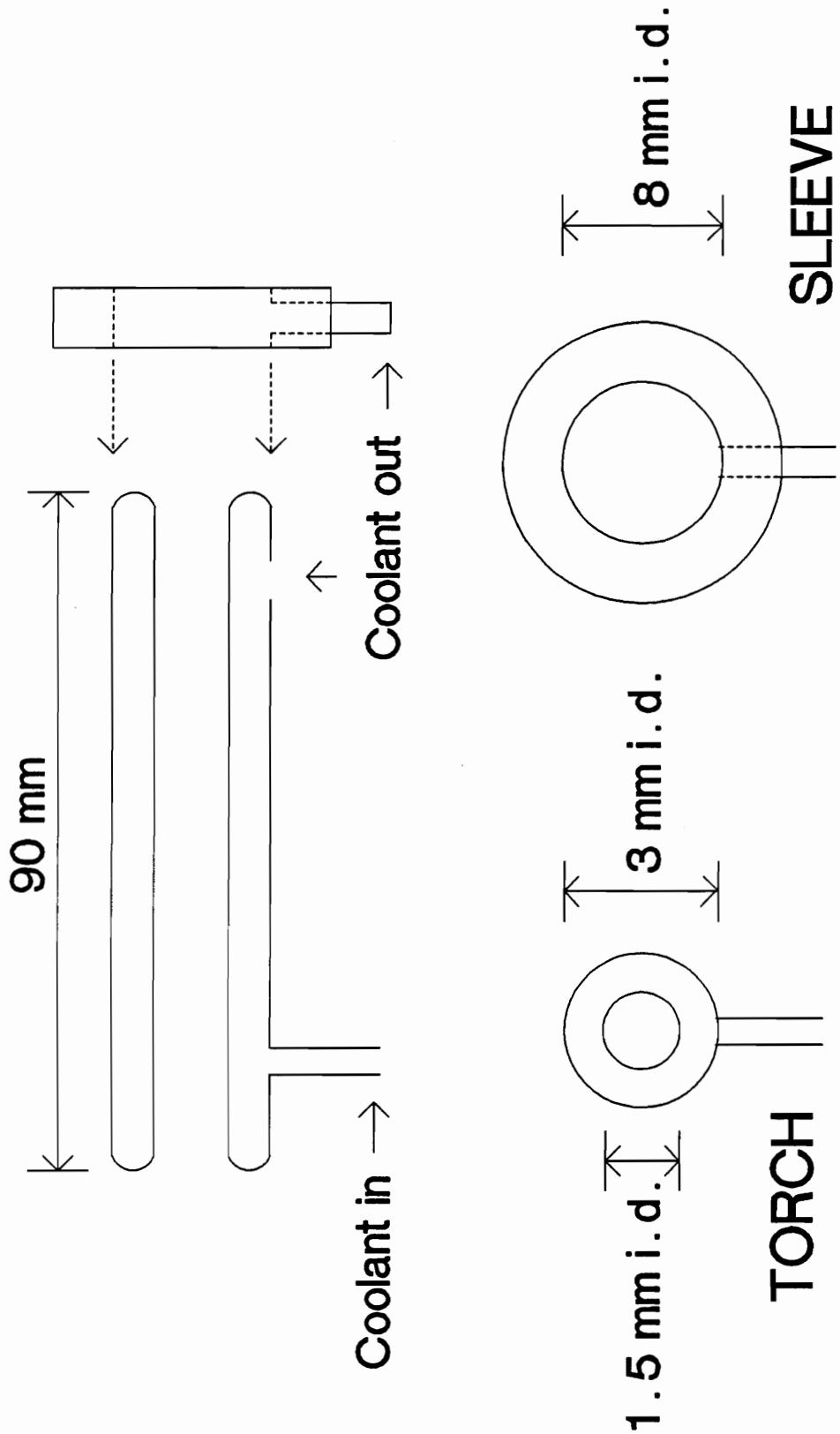

Figure A: "Cooled Torch" Design

detection was observed with this torch using a chlorine head space generator and showed great promise to address some of the limitations with the tangential flow torch. Additionally, diffusion pump oil 704 is thought to be a better coolant because its viscosity is conducive to pumping and the silicone based fluid would be thermally stable and less likely to decompose due to heat.

VITA

Curtis Bobby Motley
March 18, 1964
Franklin County, VA

EDUCATIONAL RECORD

Ph.D., Analytical Chemistry - May 1990
Virginia Polytechnic Institute and State University
Dissertation Advisor: Dr. Gary L. Long
Dissertation Topic: The Evaluation of an Argon and Helium Highly Efficient Microwave Induced Plasma as an Element Selective Detector for Packed Column Supercritical Fluid Chromatography

B. S., Chemistry, Virginia Commonwealth University, May 1986
A. S., Ferrum College, May 1984
Franklin County High School, June 1982

PUBLICATIONS

S. C. Rutan and C. B. Motley, "Factor Analysis and Kalman Filter Studies of Severely Overlapped Amino Acid Derivatives in Thin-Layer Chromatography," Anal. Chem., 59, 2045 (1987).

C. B. Motley, M. Ashraf-Khorassani and G. L. Long, "Microwave Induced Plasma as an Elemental Detector for Packed Column Supercritical Fluid Chromatography," Appl. Spectrosc., 43, 737 (1989).

C. B. Motley and G. L. Long, "Evaluation of Sample Introduction Techniques of Packed Column SFC into a MIP" Appl. Spectrosc., May 1990.

C. B. Motley and G. L. Long, "Evaluation of a He-HEMIP as an Element Selective Detector for SFC," JAAS, in press.

PRESENTATIONS

C. B. Motley and S. C. Rutan, "Computer Assisted Studies of Derivatives of Amino Acids," Eighteenth Annual Southeastern Regional Meeting of the Student Affiliates of the ACS, 1986.

S. C. Rutan and C. B. Motley, "Factor Analysis Assisted Studies of Amino Acid Derivatives," Thirteenth Meeting of the Federation of Analytical Chemistry and Spectroscopy Societies, September 1986, Paper 622.

S. C. Rutan, D. Gerow, G. H. Hartmann and C. B. Motley, "Mathematical Methods for Enhancement of Fluorescence Spectroscopic Detection for Chromatography," Eastern Analytical Symposium, New York, September 1987.

L. D. Perkins, C. B. Motley and G. L. Long, "MIP-AFS: An Update," Fourteenth Meeting of the Federation of Analytical Chemistry and Spectroscopy Societies, September 987, Paper 288.

C. B. Motley, L. D. Perkins and G. L. Long, "The Evaluation of SFC for Sample Introduction into the MIP," Pittsburgh Conference on Analytical Chemistry and Applied Spectroscopy, March 1988, Paper 042.

C. B. Motley, M. Ashraf-Khorassani, L. T. Taylor and G. L. Long, "The Evaluation of SFC Analytical Parameters with Respect to MIP Emission Spectrometry," Pittsburgh Conference on Analytical Chemistry and Applied Spectroscopy, March 1989, Paper 1111.

C. B. Motley and G. L. Long, "Evaluation of a He-HEMIP as a Detector for SFC" Sixteen Meeting of the Federation of Analytical Chemistry and Spectroscopy Societies, October 1989.

C. B. Motley and G. L. Long, "Evaluation of a He-HEMIP as an Element Selective Detector for SFC," 1990 Winter Conference on Plasma Spectrochemistry, January 1990.

C. B. Motley and G. L. Long, "Evaluation of a Helium-HEMIP as an Element Selective Detector for SFC," Pittsburgh Conference on Analytical Chemistry and Applied Spectroscopy, March 1990.

ACADEMIC HONORS AND AWARDS

Freshman Chemistry Award (1983)
Achievements in Religion (1983)
Mathematics Award (1984)
Phi Theta Kappa Honors Fraternity (1983)
Who's Who Among American Junior Colleges and Universities (1984)
Analytical Chemistry Award (1985)
American Chemical Society Student Affiliate Chapter President (1985-1986)
Phi Lambda Upsilon Honors Fraternity (1987)

ORGANIZATIONS

American Chemical Society (ACS)
Society of Applied Spectroscopy (SAS)

PRESENT EMPLOYER:

The Procter & Gamble Company
Hair and Skin Care Technology
Miami Valley Laboratories
Cincinnati, Ohio 45239